Journal of
Medicinal Chemistry

Article

New rigid nicotine analogs, carrying a norbornane moiety, are potent agonists of #7 and #3* nicotinic receptors

Dina Manetti, Alexandra Garifulina, Gianluca Bartolucci, Carla Bazzicalupi, Cristina Bellucci, Niccolò Chiaramonte, Silvia Dei, Lorenzo Di Cesare Mannelli, Carla Ghelardini, Paola Gratteri, Ekaterina Spirova, Irina Shelukhina, Elisabetta Teodori, Katia Varani, Victor Tsetlin, and Maria Novella Romanelli

J. Med. Chem., **Just Accepted Manuscript** • DOI: 10.1021/acs.jmedchem.8b01372 • Publication Date (Web): 25 Jan 2019

ACS Publications

is published by the American Chemical Society. 1155 Sixteenth Street N.W., Washington, DC 20036

New rigid nicotine analogs, carrying a norbornane moiety, are potent agonists of α7 and α3* nicotinic receptors

Dina Manetti,[a,*] Alexandra Garifulina,[b] Gianluca Bartolucci,[a] Carla Bazzicalupi,[c] Cristina Bellucci,[a] Niccolò Chiaramonte,[a] Silvia Dei,[a] Lorenzo Di Cesare Mannelli,[d] Carla Ghelardini,[d] Paola Gratteri,[e] Ekaterina Spirova,[b] Irina Shelukhina,[b] Elisabetta Teodori,[a] Katia Varani,[f] Victor Tsetlin,[b] Maria Novella Romanelli[a]

[a] Department of Neuroscience, Psychology, Drug Research and Child's Health (NEUROFARBA), Section of Pharmaceutical and Nutraceutical Sciences, University of Florence, Via Ugo Schiff 6, 50019 Sesto Fiorentino, Italy

[b] Department of Molecular Basis of Neurosignaling, Shemyakin-Ovchinnikov Institute of Bioorganic Chemistry, Russian Academy of Sciences, Miklukho-Maklaya str. 16/10, 117997 Moscow, Russia

[c] Department of Chemistry "Ugo Schiff", University of Florence, via della Lastruccia 3, 50019 Sesto Fiorentino.

[d] Department of NEUROFARBA, Section of Pharmacology and Toxicology, University of Florence, Viale G Pieraccini 6, 50139 Firenze, Italy

[e] Department of NEUROFARBA, Laboratory of Molecular Modeling Cheminformatics & QSAR, University of Firenze, via Ugo Schiff 6, I-50019 Sesto Fiorentino, Firenze, Italy.

[f] Institute of Pharmacology, University of Ferrara, Via Fossato di Mortara 17-19, 44100 Ferrara, Italy

Abstract

A 3D-database search has been applied to design a series of *endo* and *exo* 3-(pyridin-3-yl)bicyclo[2.2.1]heptan-2-amines as nicotinic receptor ligands. The synthesized compounds were tested in radioligand binding assay on rat cortex against [^{3}H]-cytisine and [^{3}H]-methyllycaconitine (MLA) to measure their affinity for α4β2* and α7* nicotinic receptors. The new derivatives showed some preference for the α4β2* over the α7* subtype, their affinity being dependent on the *endo*/*exo* isomerism and on the methylation degree of the basic nitrogen. The *endo* primary amines displayed the lowest K_i values on both receptor subtypes. Selected compounds (**1a**, **2a**, **3a** and **6a**) were tested on heterologously expressed α4β2, α7 and α3β2 receptors, and on SHSY-5Y cells. Compounds **1a** and **2a** showed α4β2 antagonistic properties while behaved as full agonists on recombinant α7 and on SHSY5Y cells. On the α3β2 subtype, only the chloro derivative **2a** showed full agonist activity and submicromolar potency (EC_{50} 0.43 μM). The primary amines described here represent new chemotypes for the α7 and α3* receptor subtypes.

Keywords

Nicotinic acetylcholine receptor; α4β2 antagonist; α7 agonist; α3 agonist; 3D-database search; molecular modeling.

Introduction

Nicotinic acetylcholine receptors (nAChRs) are considered as attractive targets for drug design due to their involvement in many pathophysiological processes in the CNS and also in non-neuronal systems.[1-7] Several nicotinic ligands entered clinical trials, mainly for cognitive deficits associated with neurological diseases, smoking cessation and pain. Several other therapeutic applications are under study, and both agonists and antagonists may be useful depending on the targeted receptor subtype and pathology.[8]

Of the seventeen nAChR subunits cloned so far (α1-10, β1-4, γ, δ, ε) only sixteen have been found in mammalian tissues (α8 has been found only in chicken). These subunits can assemble into functional pentamers in many different ways, giving a large number of possible subtypes, the high homology between them making the design of selective ligands difficult.[8-9] The heteromeric α4β2* (* indicates the possible presence of other subunits) and the homomeric α7 receptors, the most abundant nAChRs in the CNS, are the most investigated subtypes. Some degree of selectivity for ligands targeting these two subtypes has been achieved, since structural requirements are somehow different. However, many nicotinic ligands, including compounds in clinical trials or approved for therapy, have mixed pharmacological profile: as an example varenicline (Chart 1), approved for smoking cessation, showed > 500-fold higher affinity for α4β2* over α7 receptors in binding experiments, but only 8-fold higher potency in functional assays.[10-11] In functional studies, varenicline behaved as a partial agonist on α4β2* and full agonist on α7 receptors; it is possible that both activities, as well as interaction with other subtypes, contribute to the pharmacological effects of this compound.[12-13] Other well characterized ligands have a mixed pharmacological profile, such as GTS-21, an α7 partial agonist and α4β2 antagonist,[14] tested in clinical trials to treat cognitive deficit associated with Alzheimer's disease, Attention-Deficit Hyperactivity Disorder or Schizophrenia (www.clinicaltrial.gov).

Chart 1. Structure of nicotinic ligands

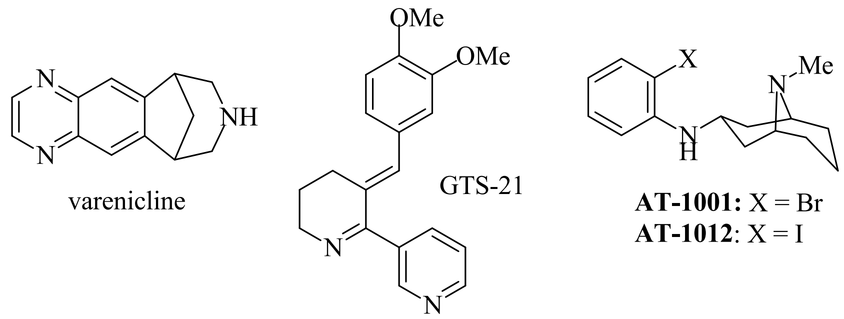

Other nAChR subtypes such as α3*, α5* and α6*, which are less abundant in the CNS,[15-16] have been studied to a lesser extent, also owing to the shortage of selective ligands. Indeed these subtypes are also attractive targets, since they are involved in neurotransmitter release or in tobacco dependence.[17-18] Moreover, the α3β4* subtype is widely expressed in the peripheral nervous system and also in non-neuronal tissues.[19] In recent times, also compounds with selectivity for α3* receptors have been discovered, such as the α3β4*partial agonists AT-1001 and AT-1012 (Chart 1); AT-1001 gave promising results when tested in rat models of nicotine or cocaine addiction.[20-21] Therefore, the design of new nicotinic modulators is still of interest.

Different strategies can be applied to search for new ligands endowed with improved activity or selectivity. Some years ago, we used a 3D database searching approach to discover novel lead compounds.[22] The requirements for the nicotinic pharmacophore, i.e. a basic nitrogen atom and an H-bond acceptor group, their distance and orientation, were extracted from pyrido[3,4]homotropane (PHT), a fully rigid α4β2 ligand (Chart 2).[23-24] These features were then transformed into a query to search within the Cambridge Structural Database (CSD), and resulted in several hits;[22] optimization of one of them resulted in quinoline analogues of nicotine.[25-26]

With the aim to find new chemotypes for the nicotinic receptors, later we repeated a similar approach, and among the retrieved hits, the molecule LOYMOB (Chart 2) gave us the idea of using a simple bicyclo[2.2.1]heptane moiety as a spacer between the pyridyl ring (H-bond acceptor) and an aliphatic amino group (see compounds with general formula **A**). These molecules possess 4 stereogenic centres, leading to 4 possible diasteromeric racemates; however, only the *trans* derivatives shown in Chart 2 would comply with the criteria of nicotinic pharmacophore. In fact, in these *trans* isomers, differing in *endo/exo* arrangement of the amino group, the distance between the basic and the pyridyl nitrogen atoms is in the range of 4.9 - 5.6 Å, in accord with the well-known nicotinic pharmacophoric models.[27] Therefore, a series of amines were designed (**1a-b** – **6a-b**), differing in the *endo* (**a**) or *exo* (**b**) arrangement of the amino group, the presence of a Cl atom on the pyridyl ring, and the number of methyl groups on the amino moiety (0-2).

Chart 2. Design of compounds **1-6** from the lead PHT.

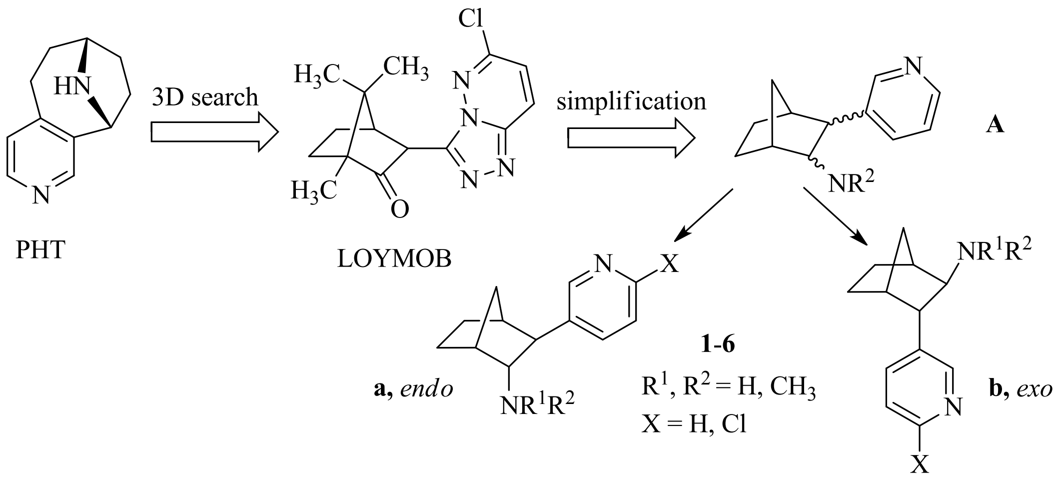

In this preliminary work we intended to assess the nicotinic potentiality of this new scaffold, leaving to a future time the optimization and the study of enantioselectivity. In fact, the norbornane ring is a structural feature also found in mecamylamine, a non competitive nicotinic antagonist, but we reckoned that the presence on the molecule of a pyridyl ring could allow the interaction with the orthosteric site, and possibly introduce agonistic properties. In addition, we were aware that the extraction from PHT of only the essential pharmacophoric features for binding to the nicotinic receptor could give new molecules which may not show subtype selectivity, since other important properties such as shape and volume have not been taken into account in the initial design.

Knowing these limitations, the designed compounds were synthesized and tested for their affinity on α4β2* and α7* nicotinic receptors of rat brain. Since some of the new compounds displayed interesting affinity, their functional properties were also assessed in vitro in SHSY5Y cells and on the heterologously expressed individual α4β2, α7 and α3β2 subtypes.

Methodology and results

3D search and design

The pharmacophoric search was performed on the Cambridge Structural Database (CSD).[28] The queries, showed in Figure 1, contained the geometrical features expected for a nicotinic agonist, i.e. a nitrogen atom, potentially cationic, and another heteroatom (as a pyridyl N, or a carbonyl O) as H-bond acceptor group. Some changes were introduced with respect to the first approach:[22] 1) the H-bond acceptor moiety could be also an oxygen atom; 2) the distance between the two pharmacophoric heteroatoms has been defined without the addition of a "dummy" lone pair; 3) the distance ranges were chosen larger than those previously reported, in order to explore either flexible structures, or the so called "water-extension" concept, which suggests the bridging role of a water molecule in the binding of ligands to the receptor.[27, 29-30] R factor ≤ 0.05 was used as an additional filter to reduce the number of structures for consideration.

From the resulted hit list we have chosen LOYMOB (Chart 2): this molecule shows a carbonyl group as H-bond acceptor moiety, while the aromatic heterocycle could be replaced with (cyclo)alkyl groups carrying or incorporating a basic nitrogen. However, we realized that there could be other ways to modify this molecule: we replaced the aromatic ring with a pyridine moiety, transformed the keto function into an amine, and removed the methyl groups on the norbornane ring, leading to compounds with general formula **A** (Chart 2). By this way, the two pharmacophoric moieties, a pyridine ring and a basic nitrogen, would be linked by a rigid spacer, the bicyclo[2.2.1]heptane ring.

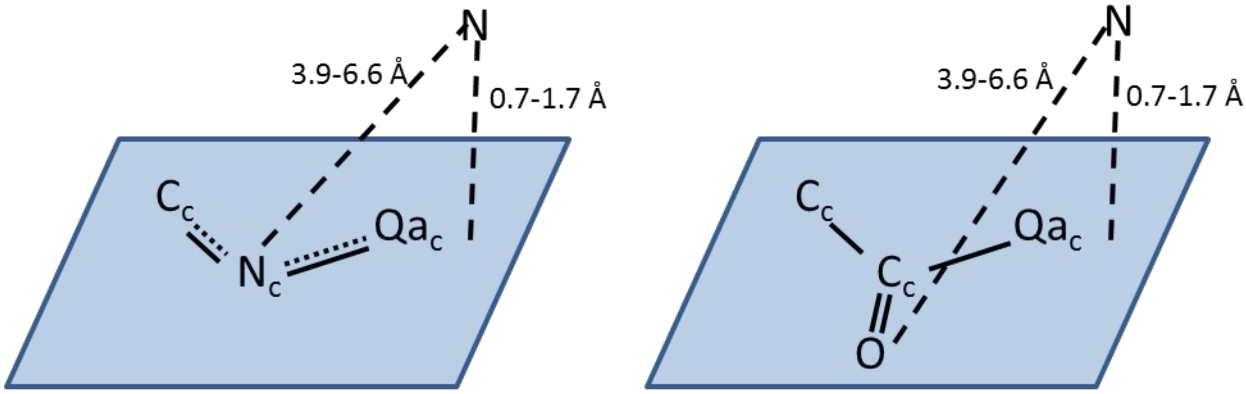

Figure 1. Queries used in the CSD search: Qa = N,C; c subscript indicates atoms belonging to rings.

Before the 3D structure of α4β2 nAChR X-ray structure was published in 2016 (XRD)[31] and, more recently in 2018 (cryo-EM),[32] comparative modeling was used by some of us to build the three-dimensional model of the N-terminal extracellular portion (Ligand Binding Domain, LBD) of the α4β2 nicotinic receptor.[33] When our work started, this was the only chance to predict the binding ability of the designed compounds. This model was used to test possible interactions of compound **1a** and **1b** (see structure in Table 1) at the binding site formed by the α4 ((+) side) and β2 ((-) side) subunits. Hydrogen bond, electrostatic and cation-π interactions with α4Y204 and α4W156 (residue numbers according to 5KXI[31]) stabilize the cationic head of compounds **1a** and **1b** while the pyridine ring extends in a hydrophobic cavity lined by residues from both subunits (Figure S1, Supporting Information). The computational study predicted that **1a** and **1b** could have high affinity for the α4β2 receptor, thus validating our design.

Chemistry

The key intermediates of the synthetic pathway were (*E*)-3-(2-nitrovinyl)pyridine **9**[34] and (*E*)-2-chloro-5-(2-nitrovinyl)pyridine **10**;[35] these compounds were synthesized by addition of nitromethane to the commercially available aldehydes, followed by dehydration of the alcoholic intermediates **7** and **8**, according to Duursma[36] (Scheme 1). Then, a Diels-Alder reaction of **9** and

10 with cyclopenta-1,3-diene, obtained after thermal decomposition and distillation of commercially available dicyclopentadiene,[34] gave compounds **11** and **12**.

Scheme 1. Synthesis of *endo* and *exo* 3-(pyridin-3-yl)bicyclo[2.2.1]heptan-2-amines 1a,b-6a,b[a]

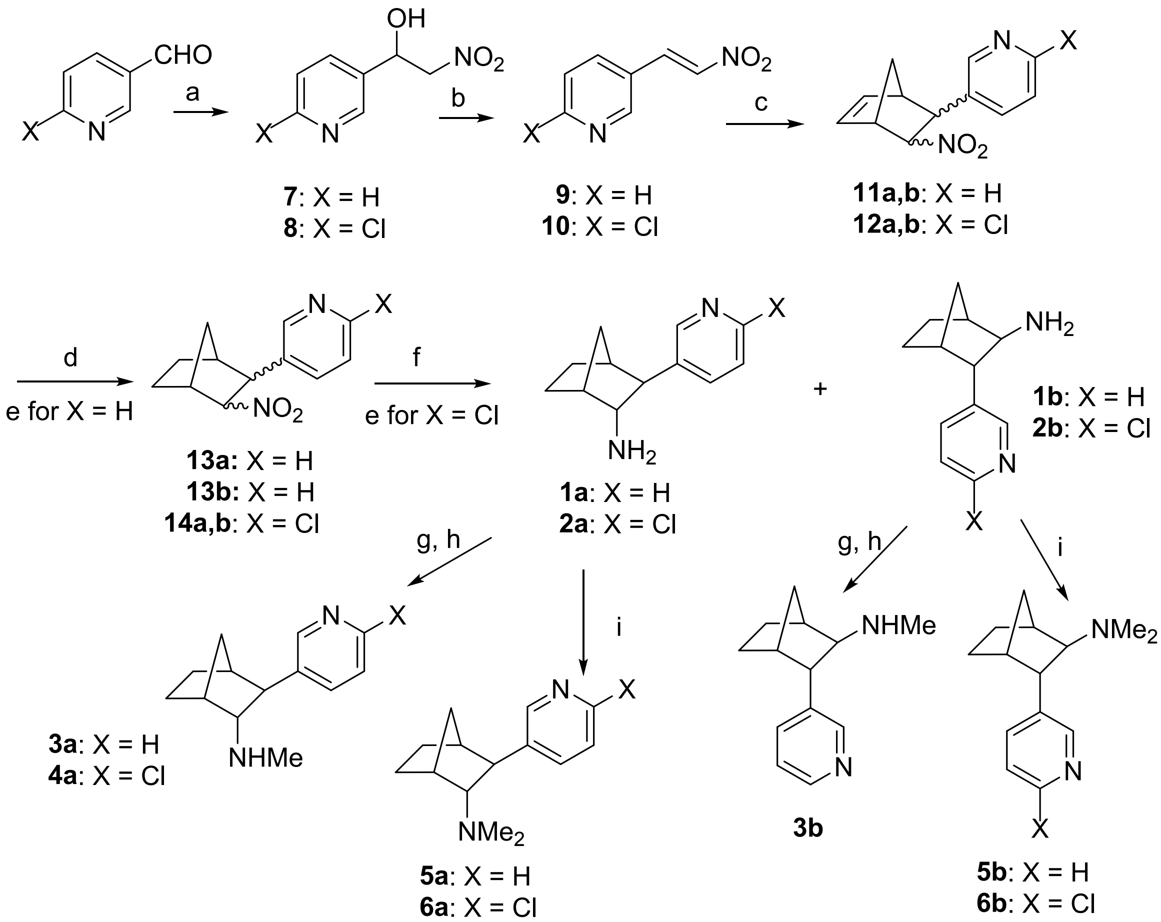

[a]Reagents and conditions: (a) CH_3NO_2, tBuOK, tBuOH; (b) $(CF_3CO)_2O$, Et_3N, -10°C; (c) cyclopenta-1,3-diene, CH_2Cl_2; (d) H_2/Pd/C; abs EtOH; (e) chromatographyc separation; (f) $SnCl_2.2H_2O$, abs EtOH, D; (g) ClCOOEt, Et_3N, CH_2Cl_2; (h) $LiAlH_4$, THF; (i) HCOOH, HCHO, abs EtOH.

The Diels-Alder reaction gave *endo*/*exo* mixtures, where the thermodynamically more stable *endo* adduct was always the predominant isomer. The two isomers were clearly visible from the NMR spectra: in fact, in the *endo* isomers, the proton geminal to the nitro group appears as a triplet at 4.97 ppm for **11a** and at 4.91 ppm for **12a**. On the contrary, in the *exo* isomer the same proton appears as a doublet at higher fields (4.52 ppm for **11b** and 4.45 ppm for **12b**). The isomeric ratios and the overall yield were dependent on the solvent used: the Diels-Alder reaction performed on **9** in toluene, 1,4-dioxane or dichloromethane gave *endo*/*exo* mixtures in 4.3:1 (68% yield), 7:1 (97% yield) and 6.4:1 (99% yield), respectively. The substituent on the pyridine nucleus had also a small effect: in dichloromethane the *endo*/*exo* ratios were 6.4:1 and 5.3:1 for **11** and **12**, respectively.

Catalytic hydrogenation of the double bond of **11a,b** and **12a,b** gave compounds **13a,b** and **14a**,**b**, respectively;[37] chromatographic separation was possible only on the former, giving **13a** and **13b**. Reduction of nitro group with $SnCl_2$ in abs ethanol,[38] and chromatographic separation gave the desired primary amines **1a, 2a,** and **1b**, **2b**. Reaction with ethyl chloroformate, followed by reduction of the intermediate carbamates gave monomethyl derivatives **3a, 3b** and **4a**; these reactions were not performed on **2b**, due to its low amount. Reaction with formaldehyde and formic acid on **1a**, **1b**, **2a** and **2b** gave tertiary amines **5a**, **5b**, **6a** and **6b**.

For biological tests, all compounds were transformed into the HCl salts.

Radioligand binding studies on rat brain.

To evaluate their affinity for the neuronal nAChRs, the synthesized compounds were tested in vitro on rat brain in competition binding experiments according to a previously applied protocol [26]; the results are reported in Table 1. [^{3}H]-Cytisine was used to detect binding to the α4β2* receptor, while [^{3}H]-methyllycaconitine (MLA) allowed to measure the interaction with the α7* subtype. Nicotine and MLA were taken as reference compounds.

As a general remark, amines **1-6** were more active on α4β2* than on α7* nicotinic receptors. The K_i values of all compounds were in the nanomolar range for the α4β2* subtype, while for some of them (**1b**, **3b**, **5a**, **5b**, **6a** and **6b**) the affinity constants were not calculated on the α7* subtype, since at 1 μM concentration the amount of displaced [^{3}H]-MLA from rat midbrain was below 33%. Some compounds displayed also a moderate selectivity: the *endo* secondary amines **3a** and **4a** showed, respectively, a 34- and 37-fold higher affinity on α4β2* than on α7* nicotinic receptors.

Endo-*exo* isomerism plays a crucial role in binding affinity: on both subtypes the *endo* compounds **1a**, **2a**, **3a**, **5a** and **6a** showed higher affinity than their *exo* isomers **1b**, **2b**, **3b**, **5b** and **6b**; potency ratios ranged, on the α4β2* subtype, from 7 for **6a**-**6b**, to 79 for **1a**-**1b**; on α7* nicotinic receptors the highest difference (22 times) was for **2a**-**2b**. *Endo*-*exo* isomers differ in the spatial orientation of the bicycloheptane moiety (shown in Figure 2), suggesting a limited space available within the binding site for the bulky spacer.

As far as methylation on the basic nitrogen atom is concerned, primary amines were more potent than secondary and tertiary ones, in both *endo* and *exo* series; on the α7 subtype, tertiary amines **5a,b** and **6a,b** showed poor interaction. Methylation affected also subtype selectivity: as mentioned before, *endo* secondary amines **3a** and **4a** showed the highest selectivity ratios, while in the *exo* series, the primary amine **2b** showed the highest preference for α4β2* over α7* receptors (8 times). This rank order of affinity is somehow unexpected, since removal of N-methyl groups of nicotinic ligands often resulted in a lower activity.[39] N-methylation should influence basicity and, as a consequence, the extent of protonation of the amino group, but the prediction of pKa values (see below) suggests for all amines a degree of protonation >99%.This detrimental effect of methylation on the activity can be explained by an increase of steric hindrance, which is better tolerated on α4β2 rather than on α7 receptors. However, the presence of more than one NH^+ moiety can give additional interactions. In fact, while testing protonated secondary amines, Post et al found evidence for a double involvement of the ammonium group, which established $NH^{+}\cdots\pi$ interactions not only with the tryptophan residue in loop B but also with a tyrosine residue in loop C.[40] These authors suggested that a smaller cation head could allow for stronger interactions with loop C in the binding site, an hypothesis that could explain also the results of this study.

The insertion of a 6-Cl atom on the pyridine ring increased the affinity for both α4β2* and α7* subtypes, even if the increment was small. The highest increase was found for the *exo* primary amine **2b** on both α4β2* ($Ki_{\mathbf{1b}}/Ki_{\mathbf{2b}}$ = 6) and α7* ($Ki_{\mathbf{1b}}/Ki_{\mathbf{2b}}$ >4). The small increase in affinity slightly enhanced selectivity (compare **2b**-**1b**, **4a**-**3a**, **6a**-**5a** and **6b**-**5b**), with the exception of primary amine **2a**: the $Ki_{\alpha7*}/Ki_{\alpha4\beta2*}$ ratio for this compound was 8, while that of the unsubstituted compound **1a** was 22.

Table 1: Binding affinity of compounds **1-6** on α4β2* and α7* receptors of rat brain, and functional activity of compounds **1a**, **2a**, **3a** and **6a**.

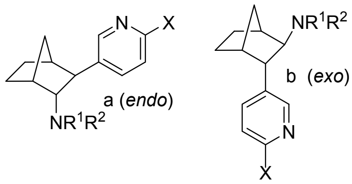

N	X	R[1]	R[2]	α4β2* K_i (nM)[a]	α7* K_i (nM)[b]	K_i (α7)/ K_i (α4β2)	hα7[c] EC_{50} (μM)	rα7[d] EC_{50} (μM)	hα3β2[e] EC_{50} (μM)	SH-SY5Y cells[f] EC_{50} (μM)
1a	H	H	H	2.11 ± 0.18	46.0 ± 4.0	22	0.048 ±0.013	5.98 ±1.50	6.32 ±1.07	1.92 ±0.66
1b	H	H	H	166 ± 14	>1000 [30%]	> 6				
2a	Cl	H	H	1.31 ± 0.19	10.53 ± 1.12	8	0.024 ±0.006	2.71 ±0.30	0.43 ±0.10	0.22 ±0.04
2b	Cl	H	H	28 ± 2	227 ± 24	8				
3a	H	H	CH_3	10.22 ± 1.09	352 ± 32	34	2.29 ±0.94	>10	65.53 ±5.74	N.d.
3b	H	H	CH_3	206 ± 18	>1000 [15%]	> 5				
4a	Cl	H	CH_3	3.12 ±0.27	116 ± 12	37				
5a	H	CH_3	CH_3	59 ± 6	>1000 [8%]	> 17				
5b	H	CH_3	CH_3	554 ± 49	>1000 [6%]	> 2				
6a	Cl	CH_3	CH_3	43 ±4	>1000 [33%]	> 23	6.45 ±0.41	>10	2.86 ±0.17	N.d.
6b	Cl	CH_3	CH_3	294 ±28	>1000 [18%]	> 3				
Nicotine				2.31 ± 0.19	-	-	4.71 ±1.44[g]			22.47±3.06
Methyllycaconitine				-	1.42± 0.17	-				

[a] Displacement of [^{3}H]-cytisine from rat cerebral cortex; K_i values are expressed as mean ±SEM (n = 4 indipendent experiments). [b] Displacement of [^{3}H]-MLA from rat midbrain; K_i values are expressed as mean ±SEM (n = 4 indipendent experiment). Square brackets: % inhibition of [^{3}H]-MLA binding at 1 μM. [c] Increase in intracellular [Ca^{2+}] on Neuro2a cells expressing hα7 receptor, in the presence of PNU 120596 (10 μM). [d] Electrophysiology on *Xenopus* oocytes, expressing rat α7 nAChR. [e] Electrophysiology on *Xenopus* oocytes, expressing human α3β2 nAChR [f] Increase in intracellular [Ca^{2+}] on SH-SY5Y cells. [g] From ref.[41]. N.d: not determined.

Molecular modeling

The binding ability of the synthesized compounds was analyzed using the X-ray structure of the human α4β2 nicotinic receptor,[31] by means of docking simulations. Compounds **1a** and **1b** were taken as representatives for all the derivatives reported in Table 1. Since these derivatives have been tested only as racemates, both enantiomers of each compound, i.e. (1*R*,2*R*,3*S*,4*S*)-**1a** (**1a$_1$**), (1*S*,2*S*,3*R*,4*R*)-**1a** (**1a$_2$**), (1*S*,2*R*,3*S*,4*R*)-**1b** (**1b$_1$**) and (1*R*,2*S*,3*R*,4*S*)-**1b** (**1b$_2$**, see structures in Figure S2, Supporting Information) were submitted to docking simulations. Overall, the docked compounds give rise to poses showing strong analogies with nicotine in the 5KXI crystal structure, and possibly differing in the orientation of the pyridine ring which can be tilted by 180°. The obtained poses and the selected contacts are shown in Figure 2 and Figure S3 (Supporting Information), and distances/angles for each contact are listed in Table 2.

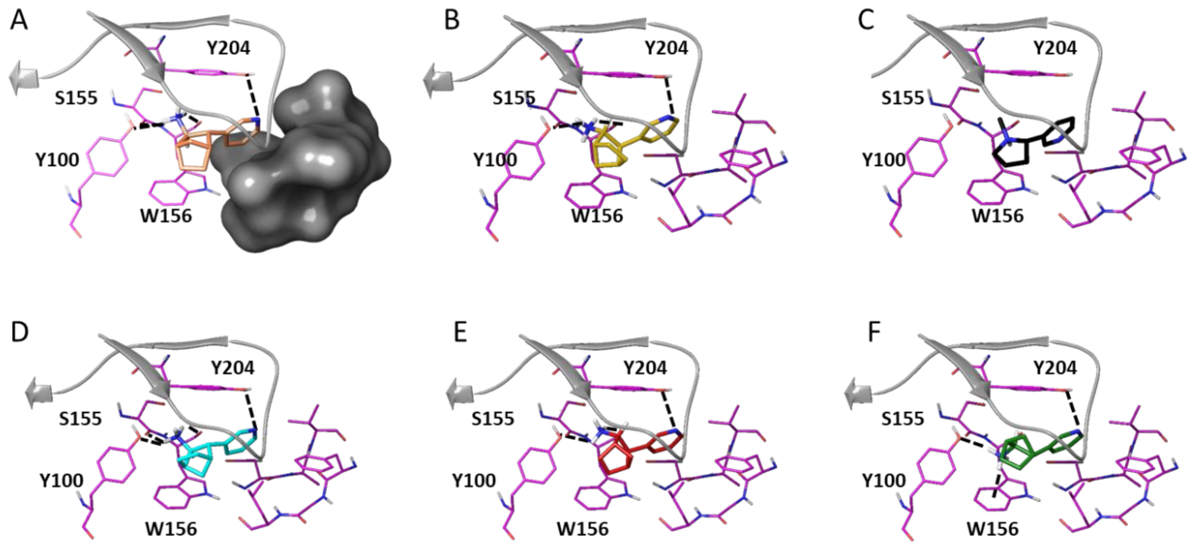

Figure 2. Predicted poses for the enantiomers of **1b** (A,B) and **1a** (D-F) in comparison with nicotine (C) (PDB 5KXI). The nitrogen atom of the pyridine ring is oriented towards α4Y204; poses with the pyridine group tilted by 180° are reported in Figure S3 (Supporting Information). (A): $\mathbf{1b_1}$;(B): $\mathbf{1b_2}$; (C): cognate nicotine in 5KXI; (D): $\mathbf{1a_1}$; (E): $\mathbf{1a_2}$ (pose I);(F): $\mathbf{1a_2}$ (pose II). The molecular surface formed by residues lining the hydrophobic pocket which accommodate the pyridine ring is shown in panel A and represented in grey.

Interestingly, the two enantiomers of compound **1b** ($\mathbf{1b_1}$ and $\mathbf{1b_2}$, *exo* configuration) gave a fairly good overlap with nicotine in the crystal structure,[31] with the position of the C - NH_3^+ group corresponding to the N – CH_3 of the nicotine. The ammonium function in all poses gives rise to H-bonds with both α4W156 and α4S155 carbonyl oxygens, as well as α4Y100 phenol oxygen. Indeed, α4W156, which is involved in the most important contacts in the nicotine complex, still plays an important role. As a matter of fact, the $NH^+\cdots\pi$ contact formed by the ligand in the X-ray structure with the indole ring of W156 (Figure 2C) is replaced in each pose of enantiomer $\mathbf{1b_1}$ by a $CH\cdots\pi$ contact (Figure 2A). The $\mathbf{1b_2}$ isomer points its CH bond towards the aromatic ring of Y204 (Figure 2B).

As far as compound **1a** (*endo* configuration) is concerned, different poses can be observed for the two enantiomers. While $\mathbf{1a_1}$ is always placed very similarly to $\mathbf{1b_1}$ (Figure 2A and 2D, Table 2), for **1a$_2$** two different poses are possible. In one of them (**1a$_2$(I)**, Figure 2E), the ammonium group still matches the position of the nicotine N-methyl group and gives the contacts previously discussed for the *exo* enantiomers **1b$_1$** and **1b$_2$**, namely the α4W156 carbonyl oxygens, the α4Y100 phenol oxygen, and the Y204 aromatic ring. On the contrary, in the other pose (**1a$_2$(II)**, Figure 2F) it does not match this position but it is involved in a very interesting $NH^{+}\cdots\pi$ contact with the indole ring of α4W156, thus restoring the pivotal π-cation interaction, and giving a possible explanation for the difference in α4β2 affinity between **1a** and **1b**. Additional considerations could be made regarding the pyridine group. Notably, in all poses found for **1a** and **1b**, the pyridine group occupies a position mostly similar to that of the same group in the nicotine crystal structure. However, some docking solutions orient the pyridine nitrogen in a similar fashion as the pyridine nitrogen in the nicotine, and, as found in the crystal structure, apparently it doesn't give any contact (Table 2, Figure 2C and Figure S3C, Supporting Information). On the other hand, the poses of Figure 2 have the pyridine group tilted by 180° and the nitrogen atom located about 3 Å apart from the phenol oxygen of α4Y204.

Therefore, the outcome of computational studies can rationalize the difference in affinity for *exo*/*endo* isomerism on the α4β2 subtype, and predicts a bifurcated H-bonds with several oxygen atoms surrounding the cationic primary amine, possibly increasing binding strength.

Table 2. Selected contacts for the pose obtained from the MM calculations

	N(py)···O d(Å)	$NH^{+}\cdots O$ d(Å)/angle DH-A(°)	$NH^{+}\cdots O{=}C$ d(Å)/angle(°)		$NH^{+}\cdots\pi$ (centroid) d(Å)
	α4Y204	α4Y100	α4W156	α4S155	α4W156
1a$_1$	-	2.2/122	2.3/137	2.9/128	-
	3.2	2.1/130	2.4/131	2.9/128	-
1b$_1$	-	2.2/155	2.3/145	3.1/131	-
	3.2	2.2/153	2.2/147	3.1/132	-

1b$_2$	-	2.1/129	2.1/142	-	-
	2.8	2.1/132	2.1/138	-	-
1a$_2$ (pose I)	-	2.6/127	2.0/149	-	-
	3.2	2.5/120	2.1/146	-	-
1a$_2$ (pose II)	-	2.5/158	2.3/136	-	2.6
	3.2	2.6/148	2.5/119	-	2.6

Calculated physicochemical properties

The calculated physicochemical properties of the compounds are reported in Table 3. Ligand efficiency (LE) has been computed by the equation of Hopkins,[42] considering the binding affinity (Ki) for α4β2* and α7*; it gives information on how efficiently a compound occupies the binding site. As reported in Table 3, all the new derivatives possess LE values in the range 0.53-0.85 Kcal/mol for the α4β2* and 0.59-0.73 Kcal/mol for the α7* subtype On the latter, LE was calculated only for compounds showing a K_i value. These values are higher than the mean value (0.45) calculated for oral drugs [43]

A series of physicochemical properties involved in the CNS penetration were also calculated, such as molecular weight (MW), polar surface area (PSA), basicity on the aliphatic (pKa1) and aromatic (pKa2) nitrogen atoms, and lipophilicity (clogP). All derivatives have a MW<270 Da and PSA< 40 Å^2. ClogP is in the range 1.7-3.2; however, according to Ghose[44] only compounds **2a**, **2b**, **4a**, **5a**, **5b**, **6a** and **6b** have lipophylicity values predictive of a good blood-brain barrier penetration (suggested range: 2.1-4-4). The logBB evaluation, as calculated by Clark[45] combining the two variables PSA and clogP, predicts that primary amines (logBB< 0) may have a medium distribution to the brain, while compounds as **6a**/**6b** with logBB >0.3 should readily cross the blood-brain barrier.[46]

Table 3. Calculated physicochemical properties of compounds **1-6**

N	LE α4β2* [Kcal/mol]	LE α7* [kcal/mol]	MW [Da]	clogP	PSA [Å²]	logBB	pKa1/pKa2
1a	0.85	0.72	188.13	1.703	38.91	-0.178	10.03/3.74
1b	0.66	-	188.13	1.703	38.91	-0.178	10.03/3.74
2a	0.81	0.73	222.09	2.500	38.91	-0.056	10.03/-0.30
2b	0.69	0.60	222.09	2.500	38.91	-0.056	10.03/-0.30
3a	0.73	0.59	202.14	1.849	24.92	0.051	10.32/3.54
3b	0.61	-	202.14	1.849	24.92	0.051	10.32/3.54
4a	0.73	0.59	236.10	2.646	24.92	0.172	10.29/-0.50
5a	0.62	-	216.16	2.385	16.13	0.262	9.81/4.17
5b	0.53	-	216.16	2.385	16.13	0.262	9.81/4.17
6a	0.59	-	250.12	3.182	16.13	0.383	9.77/0.13
6b	0.53	-	250.12	3.182	16.13	0.383	9.77/0.13

LE: Ligand binding efficacy as reported by Hopkins].[42] LE= ΔG/NHEA = -RTlnKi/NHEA= 1.372*[-log Ki(mol)]/NHEA where NHEA is the number of non-hydrogen atoms. MW molecular weight and clogP were calculated from Chembiodraw Ultra 14.0. PSA Polar Surface Area and pKa1/pKa2 were calculated at www.chemicalize.org. logBB was calculated from Clark's equation:[45] logBB= -0.0148 PSA+0.152 clogP+ 0.139.

Functional studies on α4β2 receptor

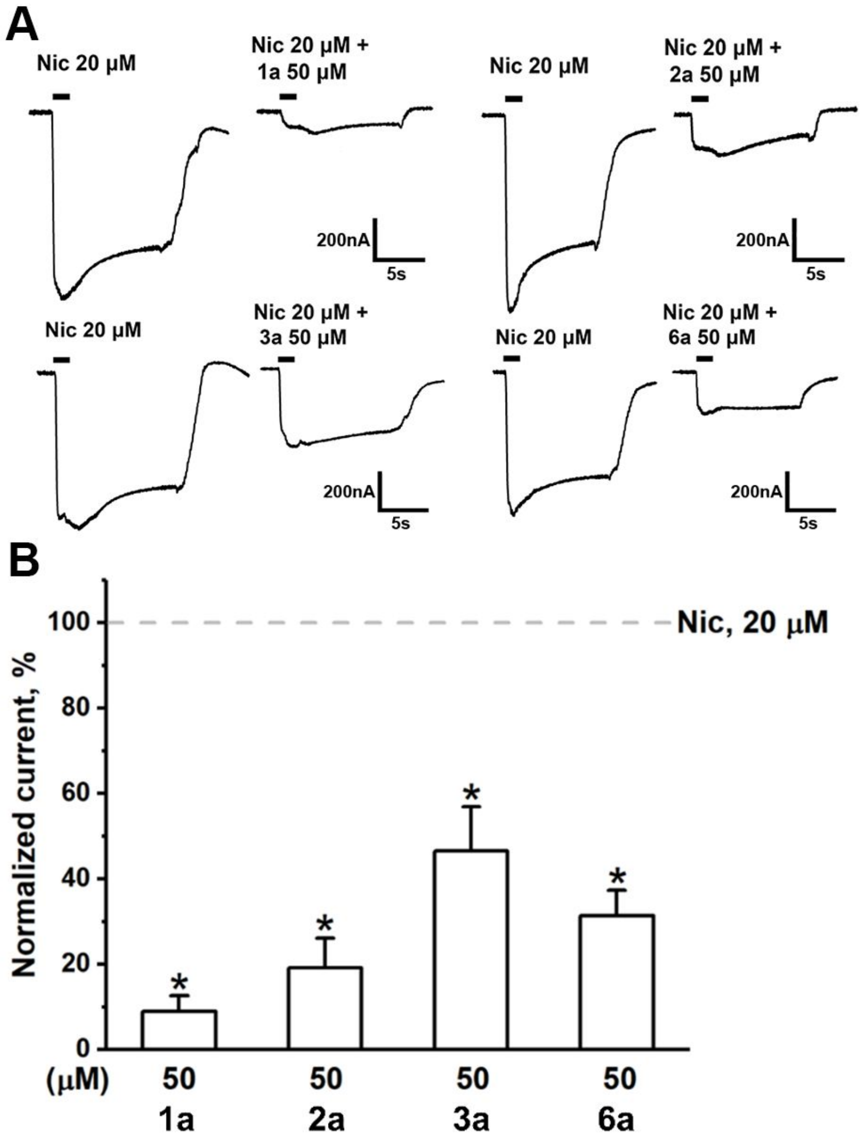

Figure 3. A) Representative nicotine (Nic)-evoked current traces mediated by human α4β2 nAChR in the presence of 50 µM of **1a**, **2a**, **3a** or **6a**. B) Bar graph for **1a**, **2a**, **3a** and **6a** (50 µM) inhibition of nicotine (20 µM)-evoked currents mediated by human α4β2 nAChR. Data are presented as mean ± SEM, n = 4 – 5. One-way ANOVA with Tukey's HSD test, *black asterisks* denote significant difference ($p < 0.05$) between normalized nicotine-evoked current in the presence of **1a**, **2a**, **3a** or **6a** and normalized nicotine-evoked current in the absence of compounds, $p = 0.00000146$

In order to measure the functional properties of the new ligands, some molecules (**1a**, **2a**, **3a** and **6a**) were chosen for further tests. Compound **2a** was selected because in the binding tests it showed the highest affinity on both subtypes, while **1a**, **3a** and **6a** were chosen for their selectivity ratios

(Table 1). Due to low availability, no *exo* isomer was selected. These compounds were tested on human α4β2 receptors expressed in *Xenopus laevis* oocytes. Two-electrode voltage clamp was used to determine their mode of action. No direct activation of human α4β2 was detected upon application of the compounds (data not shown). Application of 20 μM nicotine after 5 min incubation with the tested compounds resulted in a decrease of agonist-evoked current, revealing their antagonistic properties (Fig. 3). The most effective compounds were primary amines **1a** and **2a**, in accord with binding data (Table 1): a 50 μM concentration of these compounds was able to block 91% and 81%, respectively, of nicotine-evoked currents. Compounds **3a** and **6a** demonstrated a lower inhibitory activity on α4β2 nAChR: they were able to block 53% and 69% of nicotine-evoked currents, respectively.

Functional studies on α7 receptors

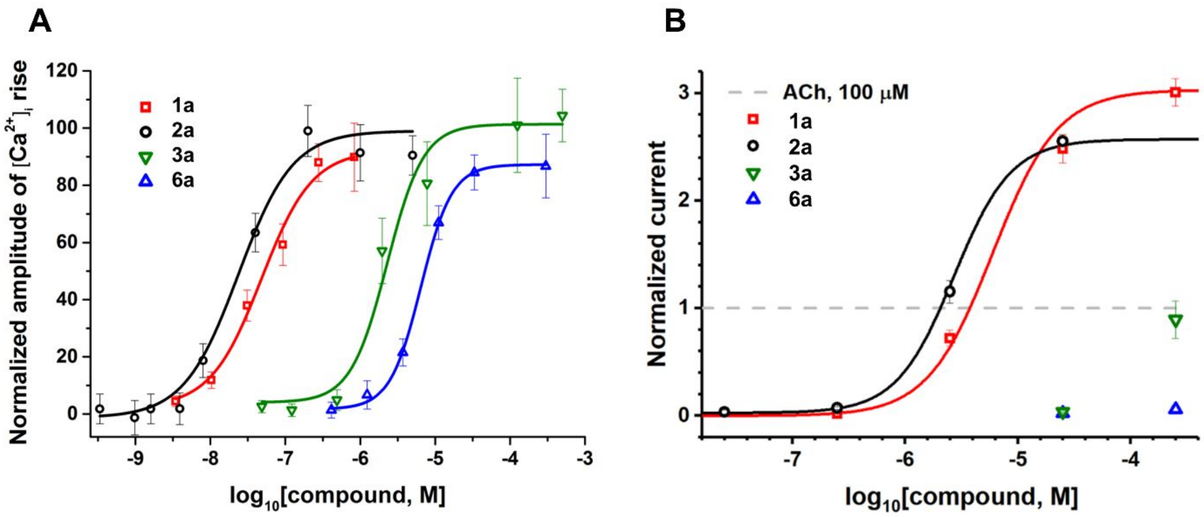

Figure 4 Functional activity of compounds **1a**, **2a**, **3a** and **6a** on α7 nAChR. A) Calcium rise of **1a** (*open red squares*), **2a** (*open black circles*), **3a** (*open green triangles*) or **6a** (*open blue triangles*) on human α7 nAChR expressed in Neuro2 cells. Peak amplitudes of compound-evoked currents were normalized to current produced by acetylcholine (100 μM). The cells were preincubated with 10 μM PNU120596, a positive allosteric modulator of α7 nAChR, for 20 minutes before agonist application. B) Agonist activity of **1a** (*open red squares*), **2a** (*open black circles*), **3a** (*open green

triangles), and **6a** (*open blue triangles*), (0.025, 0.25, 2.5, 25, 250 μM) on rat α7 nAChR expressed in *Xenopus* oocytes. Peak amplitudes of compound-evoked currents were normalized to acetylcholine (100 μM)-evoked peak current amplitude (*grey dash line*). Data are presented as mean ± SEM, n = 3. EC_{50} values are reported in Table 1.

The activity of compounds **1a**, **2a**, **3a** and **6a** was then examined on the human α7 nAChR heterologously expressed in the neuroblastoma Neuro2a cell line, where the agonist-induced increase in intracellular Ca^{2+} concentration ($[Ca^{2+}]_i$) is registered in the presence of PNU120596 (10 μM), a positive allosteric modulator (PAM).[47-50] Nicotine was taken as positive control (Fig. S4, Supporting Information). As shown in Fig. 4A, the tested compounds behaved as agonists: receptor activation, amplified by PAM co-application, produced a $[Ca^{2+}]_i$ rise, with maximal activity similar to that elicited by 100 μM ACh. Under these conditions the potency of the tested compounds was in the nanomolar (**1a** and **2a**) and micromolar (**3a** and **6a**) range (Table 1).

The agonistic properties of the compounds were further confirmed in electrophysiological assay on rat α7 receptors expressed in *Xenopus laevis* oocytes (Fig. 4B). In this test, performed in the absence of PNU120596, compounds **1a** and **2a** were full agonists, showing potency in the micromolar range (Table 1) and high efficacy: as a matter of fact, **1a** and **2a** were able to elicit a current three-times higher than that induced by 100 μM ACh (Fig. 4B). Compounds **3a** and **6a** were confirmed to be less potent also under these conditions.

Functional studies on α3β2 receptor

The agonist properties of the compounds were further tested in *Xenopus* oocytes, expressing human α3β2 nAChR (Fig. 5). In two-electrode voltage clamp experiments, all compounds were able to activate the receptor, although with different efficacy. Compound **2a** was the most potent (EC_{50} 0.43 μM) and behaved as full agonist, with maximal activity about 160% with respect to nicotine at a rather high concentration, 50 μM.[51] On the contrary, **1a** was a partial agonist showing maximal activity about 70% with respect to nicotine, while **3a** and **6a** activated the α3β2 nAChR only marginally.

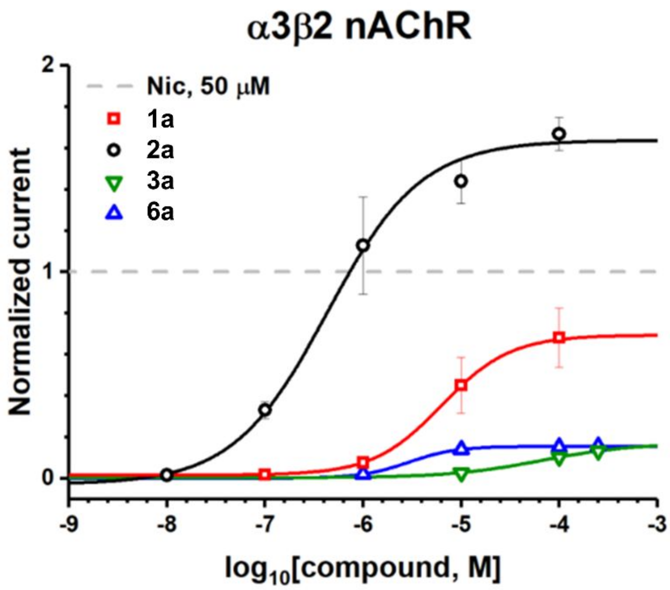

Figure 5. Agonist activity of **1a** (*open red squares*), **2a** (*open black circles*), **3a** (*open green triangles*), and **6a** (*open blue triangles*) on human α3β2 nAChR expressed in *Xenopus* oocytes. Peak amplitudes of compound-evoked currents were normalized to nicotine (50 μM)-evoked peak current amplitude (*grey dash line*). Data are presented as mean of three different oocytes ± SEM. EC_{50} values are reported in Table 1.

Functional studies on nicotinic receptors in SH-SY5Y cells

The pronounced agonistic activity of compounds **1a** and **2a** on heterologously expressed α7 and α3β2 nAChR encouraged us to check their ability to activate nicotinic receptors in human neuroblastoma SH-SY5Y cell line. This cell line endogenously expresses the α3, α5, α7, β2 and β4 subunits; according to literature data, homopentameric α7 and heteropentameric α3β2, α3α5β2, α3β2β4, α3α5β2β4, α3β4 and α3α5β4 can be present.[51] In calcium imaging experiments compounds **1a** and **2a** behaved as full agonists (Fig. 6), being able to produce a $[Ca^{2+}]_i$ rise, with EC_{50} 1.92±0.66 μM and 0.22±0.04 μM, respectively, while nicotine EC_{50} was several times higher

(22.47±3.06 μM). The chloro derivative **2a** was about 8 times more potent than the unsubstituted analogue **1a**. No increase of $[Ca^{2+}]_i$ was observed after application of **3a** and **6a**.

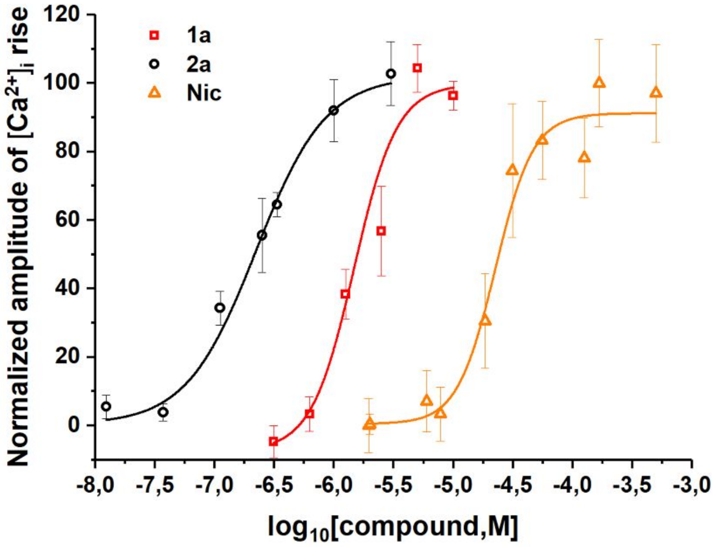

Figure 6. Agonist activity of **1a** (*open red squares*), **2a** (*open black circles*), and nicotine (*open yellow triangles*) on nicotinic receptors endogenously expressed in SH-SY5Y cells. Peak amplitudes of compound-evoked responses were normalized to response amplitude produced by nicotine (100 μM). Data are presented as mean of three independent experiments ± SEM. Each experiment includes 5-6 fluorescence measurements of one cell population (>10000 cells).

Discussion

In this work we report a new series of rigid nicotinic receptor ligands, in which the two pharmacophoric groups, the pyridyl ring and the basic amine, are separated by a bulky bicyclic spacer. The compounds represent rigid analogues of nicotine, the most potent being primary amines. It can be noticed that some primary amines have been described as high affinity α4β2 ligands;[52-56] only for few of them the interaction with the α7 subtype has been measured and found negligible.[53, 56] The *endo* primary amines reported here thus represent new chemotypes for the α7 and α3* subtypes.

The tested compounds have a mixed pharmacological profile, being antagonists at the α4β2 receptor (Fig. 3) and agonists on human and rat α7 receptors. Agonist activity towards the α7 subtype was detected in calcium-imaging experiments on Neuro2a cell line (Fig. 4) in the presence of the positive allosteric modulator PNU 120596, and confirmed also in two-electrode voltage clamp studies on the rat α7 receptors expressed in Xenopus laevis oocytes. It must be highlighted that the activity on this subtype was also revealed in competition binding experiments on rat brain, as well as by calcium imaging on the human α7 receptor in the presence of the positive allosteric modulator PNU 120596. This is important, because nicotinic receptors of the same subtype may greatly differ depending on the receptor environment; for example, the natural product 6-bromohypaphorin behaved as an agonist in the presence of PNU 120596 with the α7 receptor heterologously expressed in the Neuro2a cell line, but did not reveal agonistic properties on the chicken α7/GlyR chimera expressed in Xenopus oocytes.[57] Another factor may be the receptor species specificity: for example, α-conotoxin RgIA was considered as potential analgesic but it was found that its affinity for the human α9α10 receptor is about 100-lower than for the rat receptor.[58]

Of special interest is the activity of compounds **1a** and **2a** against α3β2 nAChR detected in electrophysiology experiments (Fig. 5). The exact role of this subtype in the CNS is not completely understood: in rodents this subtype has been found located in specific areas of CNS (habenula-interpeduncular way, cerebellum, lateral geniculate nucleus and superior colliculus).[15-16] Compounds which either potentiate or inhibit their activity are of undoubted value.

Since for a number of our compounds we detected the activities against three subtypes of nAChRs, it was of interest to check their effects on the different cell lines either of normal or malignant cells which contain the respective nAChRs in their "native " environment and may be a better approximation for assessing the suitability of these compounds as potential drugs or at least hints to drugs. We took the human neuroblastoma SH-SY5Y cell line which is known to express several nAChR subunits including α7, α3, β2. Fig. 6 shows that the increase in Ca^{+2} concentration can be induced by nicotine and, no less efficiently, by compounds **1a** and **2a**. Since without adding positive allosteric modulator PNU 120596 the α7 nAChR in this line cannot be activated,[47, 59] the increase in Ca^{+2} concentration can be ascribed to the action on the α3β2 receptor, especially in view of Fig 5, demonstrating ion currents due to activation of this heterologously expressed receptor subtype; however, the involvement of other α3* subtypes cannot be ruled out.

Conclusions

In this work we reported a series of *endo*/*exo* 3-pyridyl-bicyclo[2.2.1]heptan-2-amines, designed starting from the α4β2-selective ligand PHT. Their affinity was measured by means of binding experiments on the α4β2* and α7* receptors of rat brain. The new compounds displayed nanomolar affinity for the α4β2* subtype; on the α7* receptor the affinity was lower, but some compounds (**1a**, **2a**, **4a**) were active in the low-medium nanomolar range. On both receptor subtypes the order of potency was primary > secondary > tertiary amines, the *endo* series being more active than the *exo* one.

In electrophysiological studies, several compounds (**1a**, **2a**, **3a** and **6a**) displayed antagonistic properties on hα4β2 receptors expressed in *Xenopus laevis* oocytes, whereas calcium imaging experiments revealed agonist properties on the human and rat α7 subtypes. Interestingly, electrophysiological experiments for several compounds showed an agonistic activity towards α3β2 nAChR which agrees with their Ca^{+2} increasing concentration revealed in the neuroblastoma SH-SY5Y cells. Thus, although none of the novel synthesized primary amines possesses a strict selectivity towards one distinct nAChR subtype, still they represent a novel chemotype for several subtypes of neuronal nAChRs which also may be of value. Work is underway to probe in more detail the structure-activity relationships of this class of compounds, including enantioselectivity, in order to improve their potency and selectivity toward the α3* receptor.

Experimental Section

Chemistry

Melting points were determined on a Büchi apparatus and are uncorrected. NMR spectra were recorded on a Brucker Avance 400 spectrometer (400 MHz for ^{1}H NMR, 100 MHz for ^{13}C). ^{1}H and ^{13}C NMR spectra were measured at room temperature (25°C) in an appropriate solvent. ^{1}H and ^{13}C chemical shifts are expressed in ppm (δ) referenced to TMS. Spectral data are reported using the following abbreviations: s = singlet, bs= broad singlet, d = doublet, dd = doublet of doublets, t = triplet, app t= apparent triplet, m = multiplet, and coupling constants are reported in Hz, followed by integration. Chromatographic separations were performed on a silica gel column by gravity chromatography (Kieselgel 40, 0.063-0.2000 mm; Merck) or flash chromatography (Kieselgel 40, 0.040-0.063 mm; Merck). Analytical TLC was performed on silica gel (200-300 mesh) GF/UV 254 plates, and the chromatograms were visualized under UV light at 254 nm. Yields are given after purification, unless otherwise stated. The purity of the final compounds was determined by Agilent 1200 liquid chromatography system composed by autosampler, binary pumps, column oven and diode-array detector (LC-DAD) operating in UV range (210-400 nm). The analysis were carried out using a Phenomenex Luna PFP column 100 mm length, 2 mm internal diameter and 3 μm of particle size. The analyte separation were ensured employing as mobile phase 10 mM ammonium acetate solution (phase A) and methanol (phase B) in gradient elution. The time program elution was as follows: initial 5% phase B for 1 min, then increase to 95% phase B in 18 min and kept for 6 min. The analysis performed at constant flow of 0.35 mL min $^{-1}$, temperature of 40°C and injecting 10 μL of a 10 μg mL^{-1} solution of each analyte. The obtained results displayed that all the studied compound show a purity equal or major than 95%. The chromatographic profiles of LC-DAD analysis and corresponding UV spectra were reported in Supporting Information (Figures S6-S8, Supporting Information). High resolution mass spectrometry (HR-MS) analysis were performed with a Thermo Finnigan LTQ Orbitrap mass spectrometer equipped with an electrospray ionization source (ESI). The analysis were carried out introducing, via syringe pump at 10 μL min^{-1}, the sample solution (1.0 μg mL^{-1} in mQ water:acetonitrile 50:50), in positive ion mode. These experimental conditions allow the monitoring of protonated molecules of the studied compounds ($[M+H]^+$ species), that they were measured with a proper dwell time to achieve 60,000 units of resolution at Full Width at Half Maximum (FWHM). Elemental composition of compounds were calculated on the basis of their measured accurate masses, accepting only results with an attribution error less than 5 ppm and a not integer RDB (double bond/ring equivalents) value, in order to consider only the protonated species.[51] When reactions were performed under anhydrous conditions, the mixtures were maintained under nitrogen and the solvents were purified and dried by standard methods. Compounds were named following IUPAC rules as applied by Reaxys (version 2.19790.2) software. For biological tests, amines were transformed into the corresponding hydrochlorides, which were obtained as white solid, after crystallization from abs. ethanol/anhydrous diethyl ether.

Procedure A: synthesis of nitrovinyl pyridine (9, 10)

Step 1 (**7**, **8**). To a stirring solution of the proper aldehyde (1 equiv) in anhydrous THF (5 mL) under nitrogen, *tert*-butyl alcohol (2.8 equiv) was added at rt. After cooling at 0°C, potassium *tert*-butoxide (0.05 equiv) was added. The mixture was stirred at rt under nitrogen for 24 h; then it was quenched with a saturated water solution of NaCl and extracted with CH_2Cl_2. The organic layer was dried over Na_2SO_4 and concentrated under reduced pressure to give alcohols **7**-**8**, which were used as such for the following step.

Step 2 (**9**, **10**). To a solution of the alcohol (1 equiv) in anhydrous CH_2Cl_2 (2,5 mL), cooled at -10 °C and kept under nitrogen, trifluoroacetic anhydride (1 equiv) and triethylamine (2 equiv) were added. The mixture was stirred at -10 °C for 30 min; then it was quenched with $NaHCO_3$ (saturated solution in water) and extracted with CH_2Cl_2. The organic layer was dried over Na_2SO_4 and concentrated under reduced pressure. The crude product was purified by column chromatography using $CH_2Cl_2/CH_3OH/NH_3$ 95/6/0.8 as eluting system, to give the desired nitrovinyl pyridine.

Procedure B: Diels-Alder reaction, formation of bicyclic nucleus (11a, 11b, 12a, 12b)

To a stirred solution of (*E*)-3-(2-nitrovinyl)pyridine or (*E*)-2-chloro-5-(2-nitrovinyl)pyridine (**9-10**, 1 equiv), in anhydrous CH_2Cl_2, cyclopenta-1,3-diene (1 equiv), obtained after thermal decomposition and distillation of commercial dicyclopentadiene dymer, was added. After 72 hours stirring at rt, the solvent and the unreacted dymer were removed under reduced pressure to give the desired compound as a mixture of *endo*/*exo* isomers.

Procedure C: hydrogenation of double bond (13a, 13b, 14a, 14b)

To a stirred solution of the suitable 3-nitrobicyclo[2.2.1]heptene derivative, in absolute EtOH (20 mL), 1.3 g Pd/C (10%) were added and the mixture was hydrogenated at 27 psi for 1 h. Filtration and removal of the solvent gave a residue which was purified by chromatography or used as such for the next step.

Procedure D: reduction of nitro group (1a, 1b, 2a, 2b)

To a stirring solution of nitro derivative (1 equiv) in abs EtOH (7 mL), $SnCl_2$ $2H_2O$ (7 equiv) was added and the mixture was heated under reflux at 80 °C for 3h. After cooling, the solution was made alkaline with K_2CO_3 (saturated solution in water), filtered over celite and extracted with CH_2Cl_2. The organic layer was dried over Na_2SO_4 and concentrated under reduced pressure to give a residue that was purified by flash chromatography.

Procedure E: Amino Monomethylation (3a, 3b, 4a)

To a stirred solution of the suitable primary amine (1 equiv) in anhydrous CH_2Cl_2 (5mL) cooled at 0°C, anhydrous triethylamine (1,1 equiv) and ethyl chloroformate (1,1 equiv) were added. The mixture was stirred at rt for 24 h under nitrogen, then it was quenched with a saturated solution of Na_2CO_3 and extracted twice with CH_2Cl_2. The organic layers were dried over Na_2SO_4 and concentrated under reduced pressure to give a residue, which was used as such for the next step. The crude mixture was cooled at 0°C and, under nitrogen, treated with anhydrous THF (5 mL) and $LiAlH_4$ (2 equiv). After heating under reflux for 4h, and stirring for 12 h at rt the reaction mixture was quenched with H_2O, and NaOH (10% in H_2O) was added; the lithium salts were removed by filtration and the solution was extracted twice with CH_2Cl_2. The organic layers were dried over Na_2SO_4 and concentrated under reduced pressure. The crude product was purified by column chromatography with the appropriate eluent.

Procedure F: transformation of primary amines into N,N-dimethyl derivatives (5a, 5b, 6a, 6b)

To a stirring solution of the suitable primary amine (1 equiv) in EtOH 96% (4 mL), HCOOH (17 equiv) and CH_2O at 40% (5 equiv) were added and the solution was refluxed for 4h at 80°C. Then, the reaction mixture was alkalinized with a saturated solution of $NaHCO_3$ and was extracted with CH_2Cl_2. The organic layers were dried over Na_2SO_4 and concentrated under reduced pressure to give the desired derivative, which usually did not require further purification.

Procedure G: general procedure for the synthesis of hydrochlorides

To obtain the hydrochloride salt, an excess of acetyl chloride (2 eq for each basic nitrogen atom in the molecule) was added to anhydrous methanol (2-3 mL), then the amine (1 eq) was dissolved in this solution. After stirring for 15 min, the solvent was removed under vacuum and the solid residue was dried under vacuum and recrystallized from absolute ethanol/anhydrous diethyl ether.

endo **3-(pyridin-3-yl)bicyclo[2.2.1]heptan-2-amine (1a)**: prepared from **13a** (474.5 mg, 2.17 mmol) according to procedure D; eluent: $CH_2Cl_2/CH_3OH/NH_3$ 90/10/1. Oil (315.0 mg, 77% yield). ^{1}H NMR (400 MHz, $CDCl_3$) δ 1.24-1.43 (m, 3H, $H_{5'ax}$+ $H_{6'ax}$ + $H_{7'}$); 1.44-1.51 (m, 2H, $H_{5'eq}$+ $H_{6'eq}$); 1.53-1.65 (m, 1H, $H_{7'}$); 1.85 (d, *J*=5.2 Hz, 1H, $H_{2'}$); 2.02 (s, 1H, $H_{4'}$); 2.18 (d, *J*=3.2 Hz, 1H, $H_{1'}$); 3.00 (app t, *J*=8.4 Hz, *J*=4.4 Hz, 1H, $H_{3'}$); 7.00 (dd, *J*=8.0 Hz, *J*=5.0 Hz, 1H, H_5Ar); 7.38 (d, *J*=8.0 Hz, 1H, H_4Ar); 8.20 (d, *J*=4.4 Hz, 1H, H_6Ar); 8.32 (d, *J*= 1.6 Hz, 1H, H_2Ar). ^{13}C NMR (100 MHz, $CDCl_3$) δ 19.73 (C_7'); 30.97 (C_5'); 36.88 (C_6'); 43.30 (C_1'); 43.31 (C_4'); 55.21 (C_2'); 62.61 (C_3'); 123.19 (C_5Ar); 133.81 (C_4Ar); 141.12 (C_3Ar); 146.99 (C_6Ar); 148.44 (C_2Ar). ESI-HRMS (m/z) calculated for $[M+H]^+$ ion species $C_{12}H_{17}N_2$= 189.1386, found 189.1383.

1a.2HCl (prepared according to Procedure G): mp 145-146°C.

exo **3-(Pyridin-3-yl)bicyclo[2.2.1]heptan-2-amine (1b)**: prepared from **13b** (210.0 mg, 0.96 mmol) according to procedure D; eluent $CH_2Cl_2/CH_3OH/NH_3$ 90/10/1. Oil (54.3 mg, 30% yield).

^{1}H NMR (400 MHz, $CDCl_3$) δ 1.13-1.18 (m, 2H, $H_{5'ax}$+ $H_{7'}$); 1.23-1.27 (m, 1H, $H_{7'}$); 1.39 (d, *J*=10.0 Hz, 1H, $H_{6'ax}$); 1.56-1.61 (m, 1H, $H_{5'eq}$); 1.87 (d, *J*=9.6 Hz, 1H, $H_{6'eq}$); 2.13 (d, *J*=4.4 Hz, 1H, $H_{2'}$); 2.44 (bs, 1H, $H_{4'}$); 2.76 (bs, 1H, $H_{1'}$); 3.06 (d, *J*= 3.6 Hz, 1H, $H_{3'}$); 3.30 (bs, 2H, NH); 7.20 (dd, *J*=8.0 Hz, *J*=4.8 Hz, 1H, H_5Ar); 7.50 (d, *J*=7.6 Hz, 1H, H_4Ar); 8.41 (d, *J*=4.8 Hz, 1H, H_6Ar); 8.46 (s, 1H, H_2Ar). ^{13}C NMR (100 MHz, $CDCl_3$) δ 21.6 (C_7'); 27.07 (C_6'); 36.69 (C_5'); 42.11 (C_4'); 45.63 (C_2'); 55.44 (C_1'); 59.13 (C_3'); 123.07 (C_5Ar); 135.41 (C_4Ar); 136.66 (C_3Ar); 147.31 (C_6Ar); 149.68 (C_2Ar). ESI-HRMS (m/z) calculated for $[M+H]^+$ ion species $C_{12}H_{17}N_2$= 189.1386, found 189.1385.

1b.2HCl (prepared according to Procedure G): mp >260°C.

endo **3-(6-chloropyridin-3-yl)bicyclo[2.2.1]heptan-2-amine (2a)** and *exo*-**3-(6-chloropyridin-3-yl)bicyclo[2.2.1]heptan-2-amine (2b)**: prepared from **14a,b** (822.6 mg, 3.26 mmol) according to procedure D; after separation by column chromatography eluent: $CH_2Cl_2/CH_3OH/NH_3$ 97/3/0.3. Oils.

endo **2a** (194.3 mg, 27.0% yield): ^{1}H NMR (400 MHz, $CDCl_3$) δ 1.35-1.45 (m, 2H, CH_2); 1.48-1.53 (m, 1H, CH); 1.63-1.71 (m, 4H, NH_2+ 2CH); 1.76-1.83 (m, 1H, CH); 2.03 (app t, *J*=4.4 Hz, *J*=1.2 Hz, 1H, CH); 2.23 (s,1H, CH); 2.29 (d, *J*=3.6 Hz, 1H, CH); 3.16 (app t, *J*=4.4 Hz, *J*=4.0 Hz, 1H, CH); 7.22 (d, *J*=8.0 Hz, 1H, H_4Ar); 7.54 (dd, *J*=8.0 Hz, *J*=2.4 Hz, 1H, H_5Ar); 8.26 (d, *J*=2.4 Hz, 1H, H_2Ar). ^{13}C NMR (100 MHz, $CDCl_3$) δ 19.73 (CH_2); 31.26 (CH_2); 36.87 (CH_2); 43.33 (CH); 43.56 (CH); 54.63 (CH); 62.96 (CH); 123.89 (CH); 137.06 (CH); 140.19 (C); 148.20 (CH); 148.85 (C). ESI-HRMS (m/z) calculated for $[M+H]^+$ ion species $C_{12}H_{16}ClN_2$= 223.0997, found 223.0995.

2a.2HCl (prepared according to Procedure G): mp >260°C.

exo **2b** (17.3 mg, 2.4% yield): ^{1}H NMR (400 MHz, $CDCl_3$) δ: 1.11-1.18 (m, 2H, CH_2); 1.27-1.31 (m, 1H, CH); 1.40 (d, *J*=10.0 Hz, 1H, CH); 1.55-1.61 (m, 1H, CH); 1.62 (s, 2H, NH_2); 1.82 (d, *J*=9.6 Hz, 1H, CH); 2.07 (s, 1H, CH); 2.44 (s, 1H, CH); 2.66 (s, 1H, CH); 2.96 (d, *J*=4.0 Hz, 1H, CH); 7.24 (d, *J*=8.4 Hz, 1H, H_4Ar); 7.49 (d, *J*=8.4 Hz, 1H, H_5Ar); 8.24 (s, 1H, H_2Ar). ^{13}C NMR

(100 MHz, $CDCl_3$) δ 21.57 (CH_2); 27.06 (CH_2); 36.60 (CH_2); 41.91 (CH); 45.89 (CH); 54.93 (CH); 59.71 (CH); 123.66 (CH); 136.03 (C); 137.98 (CH); 148.86 (C); 149.38 (CH). ESI-HRMS (m/z) calculated for $[M+H]^+$ ion species $C_{12}H_{16}ClN_2$= 223.0997, found 223.0998.

2b.2HCl (prepared according to Procedure G): mp >260°C.

endo ***N*-methyl-3-(pyridin-3-yl)bicyclo[2.2.1]heptan-2-amine (3a)**: prepared from **1a** (150.0 mg, 0.8 mmol) according to procedure E; eluent: $CH_2Cl_2/CH_3OH/NH_3$ 95/6/0.8. Pale-yellow oil (80.8 mg. 50% yield). ^{1}H NMR (400 MHz, $CDCl_3$) δ 1.32-1.39 (m, 3H, $H_{5'ax}$ + $H_{6'ax}$ + $H_{7'}$); 1.61-1.69 (m, 3H, $H_{5'eq}$ + $H_{6'eq}$ + $H_{7'}$); 1.88 (bs, 1H, NH); 2.08 (dd, *J*= 5.3 Hz, *J*=1.5 Hz, 1H, $H_{2'}$); 2.21 (d, *J*=3.8 Hz, 1H, $H_{1'}$); 2.27 (s, 3H, CH_3N); 2.41 (s, 1H, $H_{2'}$); 2.98-3.00 (m, 1H, $H_{3'}$); 7.16 (dd, *J*=7.9 Hz, *J*=4.8 Hz, 1H, H_5Ar); 7.54 (d, *J*=7.9 Hz, 1H, H_4Ar); 8.36 (dd, *J*= 4.8 Hz, *J*=1.5 Hz, 1H, H_6Ar); 8.48 (d, *J*=2.2 Hz, 1H, H_2Ar). ^{13}C NMR (100 MHz, $CDCl_3$) δ 20.01 (CH_2); 31.26 (CH_2); 35.28 (CH_3); 36.23 (CH_2); 39.37 (C_4'); 43.52 (C_1'); 53.73 (C_2'); 70.20 (C_3'); 123.29 (C_5Ar); 134.24 (C_4Ar); 141.45 (C_3Ar); 147.23 (C_6Ar); 148.90 (C_2Ar). ESI-HRMS (m/z) calculated for $[M+H]^+$ ion species $C_{13}H_{19}N_2$= 203.1543, found 203.1547.

3a.2HCl (prepared according to Procedure G): low melting solid.

exo ***N*-methyl-3-(pyridin-3-yl)bicyclo[2.2.1]heptan-2-amine (3b):** prepared from **1b** (54.0 mg, 0.28 mmol) according to procedure E; eluent: $CH_2Cl_2/CH_3OH/NH_3$ 90/10/1. Oil (11.6 mg, 20% yield). ^{1}H NMR (400 MHz, $CDCl_3$) δ 1.12-1.31 (m, 3H, $H_{6'ax}$ + $2H_{7'}$); 1.42-1.45 (m, 1H, C*H*H Ax); 1.65-1.69 (m, 1H, CH*H*-Eq); 2.01 (d, *J*=8.8 Hz, 1H, CH*H*-Eq); 2.40 (s, 3H, CH_3N); 2.44 (s, 1H, $H_{4'}$); 2.48 (d, *J*=4.4 Hz, 1H, $H_{1'}$); 2.91 (d, *J*=4.4 Hz, 1H, $H_{3'}$); 3.00 (s, 1H, $H_{2'}$); 7.21-7.24 (m, 1H, H_5Ar); 7.50 (d, *J*=8.0 Hz, 1H, H_4Ar); 8.45 (d, *J*=4.8 Hz, 1H, H_6Ar); 8.47 (s, 1H, H_2Ar). ^{13}C NMR (100 MHz, $CDCl_3$) δ 21.90 (C_7'); 27.15 (CH_2); 33.11 (CH_3N); 37.42 (CH_2); 41.21 (CH); 42.85 (CH); 52.36 (C_2'); 66.76 (C_3'); 123.23 (C_5Ar); 135.31 (C_4Ar); 136.23 (C_3Ar); 147.74 (C_6Ar); 149.55 (C_2Ar). ESI-HRMS (m/z) calculated for $[M+H]^+$ ion species $C_{13}H_{19}N_2$= 203.1543, found 203.1544.

3b.2HCl (prepared according to Procedure G): low melting solid.

endo ***N*****-methyl-3-(6-chloropyridin-3-yl)bicyclo[2.2.1]heptan-2-amine (4a)**: prepared from **2a** (30.3 mg, 0.14 mmol) according to procedure E; eluent: $CH_2Cl_2/CH_3OH/NH_3$ 95/5/0.5. Oil (8 mg, 24.8% yield). ^{1}H NMR (400 MHz, $CDCl_3$) δ 1.37-1.46 (m, 3H, $H_{5'ax}$+ $H_{6'ax}$+$H_{7'ax}$); 1.63-1.75 (m, 3H, $H_{5'eq}$+ $H_{6'eq}$+$H_{7'eq}$) 1.78 (bs, 1H, NH); 2.14-2.16 (d, *J*= 8.3 Hz, 1H, CH); 2.23 (s, 1H, CH); 2.31 (s, 3H, CH_3); 2.46 (s, 1H, CH); 2.95 (s, 1H, CH); 7.24 (d, *J*=6.7 Hz, 1H, H_4Ar); 7.56 (dd, *J*=8.2 Hz, *J*=2.2 Hz, 1H, H_5Ar); 8.28 (s, 1H, H_2Ar). ^{13}C NMR (100 MHz, $CDCl_3$) δ 19.94 (CH_2); 31.20 (CH_2); 35.27 (CH_3); 36.21 (CH_2); 39.38 (CH); 43.69 (CH); 53.05 (CH); 70.43 (CH); 123.86 (CHAr); 137.29 (CHAr); 141.45 (CAr); 148.45 (CHAr); 148.85 (CAr). ESI-HRMS (m/z) calculated for $[M+H]^+$ ion species $C_{13}H_{18}ClN_2$= 237.1153, found 237.1154.

4a.2HCl (prepared according to Procedure G): low melting solid.

endo ***N,N*****-dimethyl-3-(pyridin-3-yl)bicyclo[2.2.1]heptan-2-amine (5a)**: prepared from **1a** (160.0 mg, 0.85 mmol) according to procedure F. Pale-yellow oil (164.1 mg, 89.3% yield). ^{1}H NMR (400 MHz, $CDCl_3$) δ 1.24-1.27 (dd, *J*=9.2 Hz, *J*=1.2 Hz, 1H, $H_{6'ax}$); 1.37-1.44 (m, 1H, $H_{7'}$); 1.47-1.53 (m, 1H, $H_{5'ax}$); 1.57-1.62 (m, 1H, $H_{5'eq}$); 1.71 (d, *J*= 10.4 Hz, 1H, $H_{6'eq}$); 1.81-1.88 (m, 1H, $H_{7'}$); 2.04 (d, *J*=3.2 Hz, 1H, $H_{2'}$); 2.08 (s, 6H, $2CH_3$); 2.37 (d, *J*=3.6 Hz, 1H, $H_{1'}$); 2.45-2.49 (m, 2H, $H_{3'}$ + $H_{4'}$); 7.19 (dd, *J*=8.0 Hz, *J*=4.8 Hz, 1H, C_5Ar); 7.58 (d, *J*=8.0 Hz, 1H, C_4Ar); 8.40 (d, *J*=4.4 Hz, 1H, C_6Ar); 8.53 (s, 1H, C_2Ar). ^{13}C NMR (100 MHz, $CDCl_3$) δ 21.07 (CH_2); 31.23 (CH_2); 36.34 (CH_2); 40.22 (C_3'); 45.20 (CH_3); 46.75 (C_2'); 53.16 (CH-N C_1'); 75.29 (C_4'); 123.17 (C_5Ar); 134.64 (C_4Ar); 141.82 (C_3Ar); 148.07 (C_6Ar); 150.03 (C_2Ar). ESI-HRMS (m/z) calculated for $[M+H]^+$ ion species $C_{14}H_{21}N_2$= 217.1699, found 217.1702.

5a.2HCl (prepared according to Procedure G): mp 204-205°C

exo ***N,N*****-dimethyl-3-(pyridin-3-yl)bicyclo[2.2.1]heptan-2-amine (5b)**: prepared from **1b** (27.0 mg, 0.14 mmol) according to procedure F. Oil (28.7 mg, 92.5% yield). ^{1}H NMR (400 MHz, $CDCl_3$) δ 1.13-1.24 (m, 3H, $H_{6'ax}$ + $2H_{7'}$); 1.36 (d, *J*=9.6 Hz, 1H, $H_{5'ax}$); 1.62-1.67 (m, 1H, $H_{6'eq}$); 1.90 (d, *J*=9.2 Hz, 1H, $H_{5'eq}$); 2.14 (s, 6H, $2CH_3$); 2.21 (d, *J*=4.4 Hz, 1H, $H_{2'}$); 2.33 (s, 1H, $H_{1'}$); 2.49 (d, *J*=4.4 Hz, 1H, $H_{4'}$); 2.95 (d, *J*=4.0 Hz, 1H, $H_{3'}$); 7.21 (dd, *J*=7.8 Hz, *J*=4.8 Hz, 1H, C_5Ar); 7.52 (d, *J*=7.8 Hz, 1H, C_4Ar); 8.42 (d, *J*=4.6 Hz, 1H, C_6Ar); 8.50 (s, 1H, C_2Ar). ^{13}C NMR (100 MHz, $CDCl_3$) δ 22.11 (C_7'); 27.70 (C_6'); 37.75 (C_5'); 39.78 (C_4'); 43.62 (C_1''); 43.83 (CH_3); 52.14 (C_3'); 74.04 (C_3'); 122.97 (C_5Ar); 135.47 (C_4Ar); 137.79 (C_3Ar); 147.38 (C_6Ar); 150.05 (C_2Ar). ESI-HRMS (m/z) calculated for $[M+H]^+$ ion species $C_{14}H_{21}N_2$= 217.1699, found 217.1696.

5b.2HCl (prepared according to Procedure G): mp 210-211°C.

endo ***N,N*-dimethyl-3-(6-chloropyridin-3-yl)bicyclo[2.2.1]heptan-2-amine (6a)**: prepared from **2a** (58.0 mg, 0.26 mmol) according to procedure F. Oil (56.7 mg, 86% yield). ^{1}H NMR(400 MHz, $CDCl_3$) δ 1.27-1.30 (d, *J*=10.4 Hz, 1H, $1H_{ax}$); 1.40-1.46 (m, 1H, $1H_{ax}$); 1.48-1.53 (m, 1H, $1H_{eq}$); 1.55-1.59 (m, 1H, $1H_{ax}$); 1.68 (d, *J*=10.0 Hz, 1H, $1H_{eq}$); 1.82-1.90 (m, 1H, $1H_{eq}$); 2.03 (s, 1H, CH); 2.06 (s, 6H, $2CH_3$); 2.38 (s, 1H, CH); 2.44 (s, 1H, CH); 2.47 (s, 1H,CH); 7.23 (d, *J*=8.0 Hz, 1H, H_4Ar); 7.56 (d, *J*=6.4 Hz, 1H, H_5Ar); 8.31 (s, 1H, H_2Ar). ^{13}C NMR (100 MHz, $CDCl_3$) δ 20.7 (CH_2); 31.2 (CH_2); 45.8 (CH_2); 40.24 (CH); 45.19 ($2CH_3$); 46.70 (CH); 52.48 (CH); 75.52 (CH); 123.73 (CH); 137.62 (CH); 140.82 (C); 148.92 (C); 148.98 (CH). ESI-HRMS (m/z) calculated for $[M+H]^+$ ion species $C_{14}H_{20}ClN_2$= 251.1310, found 251.1310.

6a.2HCl (prepared according to Procedure G): mp > 260 °C.

exo ***N,N*-dimethyl-3-(6-chloropyridin-3-yl)bicyclo[2.2.1]heptan-2-amine (6b)**: prepared from **2b** (15.0 mg, 0.068 mmol) according to procedure F. Oil (15.3 mg, 90% yield). ^{1}H NMR (400 MHz, $CDCl_3$) δ 1.12-1.24 (m, 2H, $1H_{ax}$ +$1H_{eq}$, CH_2); 1.25-1.32 (m, 1H, $1H_{ax}$); 1.36 (d, *J*=9.9 Hz, 1H, $1H_{ax}$); 1.62-1.69 (m, 1H, $1H_{eq}$); 1.88 (d, *J*=9.8 Hz, 1H, $1H_{eq}$); 2.14 (s, 6H, $2CH_3$); 2.15 (s, 1H, CH); 2.31 (d, *J*=10.5 Hz, 1H, CH); 2.49-2.51 (m, 1H, CH); 2.96 (s, 1H, CH); 7.25 (d, *J*=8.0 Hz, 1H, H_4Ar); 7.49 (d, *J*=8.2 Hz, 1H, H_5Ar); 8.27 (s, 1H, H_2Ar). ^{13}C NMR (100 MHz, $CDCl_3$) δ 22.11 (CH_2); 27.70 (CH_2); 37.75 (CH_2); 39.78 (CH); 43.62 (CH); 43.83 ($2CH_3$); 52.14 (CH); 74.04 (CH); 122.97 (CH); 136.93 (C); 138.46 (CH); 149.05 (C); 149.62 (CH). ESI-HRMS (m/z) calculated for $[M+H]^+$ ion species $C_{14}H_{20}ClN_2$= 251.1310, found 251.1309.

6b.2HCl (prepared according to Procedure G): mp > 260 °C.

2-Nitro-(pyridin-3-yl)ethan-1-ol (7)[60]: prepared from nicotinaldehyde (2g, 0.018 mol) according to procedure A (step 1). Oil (2.98 g, 98.5% yield). ^{1}H NMR (400 MHz, $CDCl_3$) δ 4.53-4.61 (m, 2H, CH_2); 5.50 (dd, *J*=9.6 Hz, *J*=3.2 Hz, 1H, CH); 7.33 (t, *J*=2.8 Hz, 1H, Ar); 7.80 (d, *J*=8.0 Hz, 1H, Ar); 8.44 (d, *J*=4.8 Hz, 1H, Ar); 8.50 (d, *J*=2.0 Hz, 1H, Ar).

1-(6-Chloropyridin-3-yl)-2-nitroethan-1-ol (8)[35]: prepared from 6-chloro-nicotinaldehyde (2g, 0.014 mol) according to procedure A (step 1). Oil, (2.02 g, 71% yield). ^{1}H NMR (400 MHz, $CDCl_3$) δ 3.99 (bs, 1H, OH); 4.54-4.60 (m, 2H, CH_2); 5.53 (dd, *J*=9.2 Hz, *J*=3.6 Hz, 1H, CH); 7.36 (d, *J*=8.0 Hz, 1H, H_4Ar); 7.75 (dd, *J*=8.4 Hz, *J*=2.4 Hz, 1H, H_3Ar); 8.34 (d, *J*=2.8 Hz, 1H, H_5Ar).

(*E*)-3-(2-nitrovinyl)pyridine, (9)[34]: prepared from **7** (2.98 g, 0.017 mol) according to procedure A (step 2). Pale-yellow solid, mp 145-146 °C, (1,7 g, 64% yield). ^{1}H NMR (400 MHz, $CDCl_3$) δ 7.40 (dd, *J*=7.2 Hz, *J*=4.8 Hz, 1H, Ar); 7.62 (d, *J*=13.6 Hz, 1H, *CH*=CH); 7.87 (d, *J*=7.2 Hz, 1H, Ar); 8.00 (d, *J*=13.6 Hz, 1H, C*H*=CH); 8.71 (d, *J*=4.8 Hz, 1H, Ar); 8.79 (s, 1H, Ar).

(*E*)-2-chloro-5-(2-nitrovinyl)pyridine, (10)[35]: prepared from **8** (2.02 g, 0.010 mol) according to procedure A (step 2). Pale-yellow oil (1.34 g, 73.2% yield). ^{1}H NMR (400 MHz, $CDCl_3$) δ 7.44 (d, *J*=8.0 Hz, 1H, H_4Ar); 7.60 (d, *J*=13.6 Hz, 1H, C*H*=CH); 7.82 (d, *J*=6.8Hz, 1H, H_3Ar); 7.96 (d, *J*=13.6 Hz, 1H, CH=C*H*); 8.57 (s, 1H, H_6Ar). ^{13}C NMR (100 MHz, $CDCl_3$) δ 120.89 (C); 125.13 (CH); 129.01 (C); 134.03 (CH); 137.38 (CH); 138.75 (CH); 150.33 (CH).

3-(3-nitrobicyclo[2.2.1]hept-5-en-2-yl)pyridine (11a,b)[34]: prepared from **9** (1.18g, 7.87 mmol), cyclopenta-1,3-diene (0.52 g, 7.87 mmol) and CH_2Cl_2 (8 mL) according to procedure B. Orange oil (1.68 g, 99% yield), mixture of *endo*/*exo* isomers (6.4:1). ^{1}H NMR (400 MHz, $CDCl_3$) δ 1.59 (d, *J*=9.2 Hz, 1H, $1H_{ax}$ *endo*); 1.67-1.70 (m, 2H, $1H_{eq}$ *endo* + $1H_{ax}$ *exo*); 1.98 (d, *J*=9.2 Hz, $1H_{eq}$ *exo*); 3.01 (s, 1H, CH, *endo*); 3.09 (s, 1H, CH, *exo*); 3.24 (s, 1H, CH, *endo*); 3.34 (s, 1H, CH, *exo*); 3.47 (s, 1H, CH, *endo*); 3.75 (s, 1H, CH, *exo*); 4.52 (d, *J*=3.6 Hz, 1H, $CHNO_2$, *exo*); 4.97 (app t, *J*=4.0 Hz, 1H, $CHNO_2$, *endo*); 5.97 (dd, *J*=5.6 Hz, *J*=2.8 Hz, 1H, C*H*=CH, *endo*); 6.05 (dd, *J*=5.6 Hz, *J*=2.8 Hz, 1H, C*H*=CH, *exo*); 6.12 (app t, *J*=5.6 Hz, *J*=3.2 Hz, 1H, CH=C*H*, *exo*); 6.43 (dd, *J*=5.6 Hz, *J*=3.2 Hz, 1H, CH=C*H*, *endo*); 7.05 (dd, *J*=8.0 Hz, *J*=4.8 Hz, 1H, *exo*); 7.12 (dd, *J*=8.0 Hz, *J*=4.8 Hz, 1H, *endo*); 7.24 (dd, *J*=8.0 Hz, *J*=5.2 Hz, 1H, *exo*); 7.35 (d, *J*=8.0 Hz, 1H, *exo*); 7.52 (d, *J*=7.6 Hz, 1H, *endo*); 8.32 (s, 1H *endo*); 8.45 (s, 1H *endo*); 8.62 (s, 1H, *exo*).

2-chloro-5-(3-nitrobicyclo[2.2.1]hept-5-en-2-yl)pyridine (12a,b): prepared from **10** (226.5 mg, 1.23 mmol), cyclopenta-1,3-diene (81.24 mg, 1.23 mmol) and CH_2Cl_2 (6 mL) according to procedure B. Oil (288.7 mg, 93.8% yield), mixture of *endo* /*exo* isomers (5.3:1). ^{1}H NMR (400 MHz, $CDCl_3$) δ 1.78-1.85 (m, 2H, CH_2 *endo*); 1.87 (dd, *J*= 9.2 Hz, *J*=1.6 Hz, 1H, $1H_{ax}$ *exo*); 2.14 (d, *J*=9.2 Hz, 1H, $1H_{eq}$ *exo*); 3.17 (d, *J*= 1.6 Hz, 1H, CH, *endo*); 3.24 (s, 1H, CH, *exo*); 3.38 (d, *J*=3.6 Hz, 1H, CH, *endo*); 3.53 (s, 1H, CH, *exo*); 3.65 (s, 1H, CH, *endo*); 3.89 (t, *J*=3.6 Hz, 1H, CH, *exo*); 4.45 (dd, *J*=4.4 Hz, *J*= 1.2 Hz, 1H, $CHNO_2$, *exo*); 4.91 (app t, *J*=8.0 Hz, *J*= 4.0 Hz, 1H, $CHNO_2$, *endo*); 6.15 (dd, *J*=5.6 Hz, *J*=2.8 Hz, 1H, C*H*=CH, *endo*); 6.21 (dd, *J*=5.6 Hz, *J*=2.8 Hz, 1H, C*H*=CH, *exo*); 6.29 (app t, *J*=5.6 Hz, *J*=3.2 Hz, 1H, CH=C*H*, *exo*); 6.58 (dd, *J*=5.6 Hz, *J*=3.6 Hz, 1H, CH=C*H*, *endo*); 7.26 (s, 1H, H_4Ar, *exo*); 7.30 (d, *J*=8.4 Hz, 1H, H_4Ar, *endo*); 7.46 (dd, *J*=8.4 Hz, *J*=2.4 Hz, 1H, H_3Ar, *exo*); 7.63 (dd, *J*=8.4 Hz, *J*= 2.4 Hz, 1H, H_3Ar, *endo*); 8.23 (d, *J*=2.4 Hz, 1H, H_6Ar, *exo*); 8.36 (d, *J*=2.4 Hz, 1H H_6Ar, *endo*).

endo **3-(3-nitrobicyclo[2.2.1]heptan-2-yl)pyridine (13a)** and *exo* **3-(3-nitrobicyclo[2.2.1]heptan-2-yl)pyridine (13b)**: prepared from **11a,b** (201 mg, 0.93 mmol) according to procedure C, after separation by column chromatography (hexane/AcOEt 1/1).

13a (125.7 mg, 62% yield): ^{1}H NMR (400 MHz, $CDCl_3$) δ 1.31-1.38 (m, 1H, $H_{5'ax}$); 1.48-1.59 (m, 3H, $H_{5'eq}$+ $H_{6'ax}$ + $H_{7'}$); 1.67-1.79 (m, 2H $H_{6'eq}$ + $H_{7'}$); 2.53 (d, *J*=3.3 Hz, 1H, $H_{4'}$); 2.95 (s, 1H, $H_{1'}$); 3.48 (d, *J*=2.8 Hz, 1H, $H_{2'}$); 4.74 (app t, *J*=8.2 Hz, *J*=3.8 Hz, 1H, $H_{3'}$); 7.16 (dd, *J*=7.8 Hz, *J*=4.8 Hz, 1H, H_5Ar); 7.48 (d, *J*=7.9 Hz, 1H, H_4Ar); 8.38 (d, *J*=4.2 Hz, 1H, H_6Ar); 8.45 (s, 1H, H_2Ar). ^{13}C NMR (100 MHz, $CDCl_3$) δ 22.25 (C_5'); 29.49 (C_6'); 36.78 (C_7'); 42.53 (C_4'); 42.92 (C_1'); 47.64 (C_2'); 94.16 (C_3'); 123.55 (C_5Ar); 134.21 (C_4Ar); 138.00 (C_3Ar); 148.16 (C_6Ar); 148.53 (C_2Ar).

13b (14.8 mg, 7.3% yield): ^{1}H NMR (400 MHz, $CDCl_3$) δ 1.21-1.33 (m, 2H, $H_{5'ax}$+ $H_{6'ax}$); 1.38-1.48 (m, 1H, $H_{5'eq}$); 1.59 (dd, *J*=10.5 Hz, *J*=1.4 Hz, 1H, $H_{7'}$); 1.76-1.82 (m, 1H, $H_{6'eq}$); 2.08 (dd, *J*=10.5 Hz, *J*=1.8 Hz, 1H, $H_{7'}$); 2.75-2.73 (m, 1H, $H_{4'}$); 3.01 (d, *J*=4.6 Hz, 1H, $H_{1'}$); 3.91-3.89 (m, 1H, $H_{2'}$); 4.64 (d, *J*=5.1 Hz, 1H, $H_{3'}$); 7.31 (dd, *J*=7.8 Hz, *J*=4.9 Hz, 1H, H_4Ar); 7.56 (d, *J*=7.9 Hz, 1H, H_5Ar); 8.53 (bs, 2H, H_2Ar + H_6Ar). ^{13}C NMR (100 MHz, $CDCl_3$) δ 21.79 (C_5'); 26.68 (C_6'); 37.65 (C_7'); 41.52 (C_4'); 44.25 (C_1'); 50.64 (C_2'); 91.40 (C_3'); 123.41 (C_4Ar); 134.10 (C_3Ar); 135.15 (C_5Ar); 148.30 (C_6Ar); 149.28 (C_2Ar).

2-chloro-5-(3-nitrobicyclo[2.2.1]heptan-2-yl)pyridine (14a,b): prepared from **12a,b** (631.4 mg, 2.52 mmol) according to procedure C. Oil (590.0 mg, 92.7% yield), mixture of *endo/exo* isomers (5.8:1). ^{1}H NMR (400 MHz, $CDCl_3$) δ 1.21-1.35 (m, 2H, CH_2 *exo*); 1.41-1.48 (m, 1H, 1H_{ax} *endo*); 1.60 (m, 2H, CH_2, *endo*); 1.65-1.71 (m, 1H, 1H_{ax} *exo*); 1.77-1.82 (m, 4H, 1H_{eq} +1H_{ax} *endo,* 1H_{ax} + 1H_{eq} *exo*); 2.00-2.08 (m, 2H, 1H_{eq} *endo* + 1H_{eq} *exo*); 2.61 (d, *J*= 3.6 Hz, 1H, *endo*); 2.71 (s, 1H, *exo*); 2.98 (d, *J*=4.4 Hz, 1H, *exo*); 3.06 (s, 1H, *endo*); 3.56 (d, *J*= 4.4 Hz, 1H, *endo*); 3.82 (s, 1H, *exo*); 4.55 (d, *J*=5.2 Hz, 1H, $CHNO_2$, *exo*); 4.75 (app t, *J*=4.8 Hz, 1H, $CHNO_2$, *endo*); 7.29 (d, *J*=8.0 Hz, 1H, H_4Ar, *endo*); 7.32 (d, *J*=8.4 Hz, 1H, H_4Ar, *exo*); 7.54-7.58 (m, 2H, 1H *exo* + 1H *endo*, H_3Ar); 8.28 (s, 1H, H_6Ar, *exo*); 8.30 (s, 1H, H_6Ar, *endo*).

Radioligand binding Studies

The affinity of the synthesized compounds for the α4β2* receptor was measured on rat cerebral cortex using [^{3}H]-cytisine as radioligand, according to previously published protocol.[61] The affinity of the synthesized compounds for the α7* subtype was measured on rat brain (minus cortex, striatum and cerebellum) using [^{3}H]-methyllycaconitine as radioligand, according to literature procedures. [62-63] All the assays were performed as 4 indipendent experiments in duplicate. Amines were tested as hydrochlorides.

Electrophysiology

Plasmid pcDNA3.1 construct of rat α7 nAChR subunit was linearized with *Xba*I (NEB, USA), plasmid pSP64 construct of human α4 nAChR subunit – with *BamH*I (NEB, USA), plasmid pT7TS constructs of human nAChR α3 and β2 subunit – with *Xba*I (NEB, USA); and plasmid TMEM35-pCMV6-XL5 construct with the chaperone NACHO – with *Xma*I (NEB, USA). Linearized plasmid constructs were subjected to in vitro cRNA transcription using the T7 (rat α7 nAChR, human α3 nAChR, human β2 nAChR, and NACHO) or SP6 (human α4 nAChR) mMessage mMachine® transcription kit (AMBION, USA). Stage V-VI *Xenopus laevis* oocytes were defolliculated with 2 mg/mL collagenase Type I (Life Technologies, USA) at room temperature (21-24 °C) for 2 h in Ca2+-free Barth's solution composed of (in mM) 88 NaCl, 1.1 KCl, 2.4 $NaHCO_3$, 0.8 $MgSO_4$ and 15 HEPES-NaOH at pH 7.6. Oocytes were injected with 9.2 ng of cRNAs of human α3 and β2 nAChR subunits (in a ratio 1:1), human α4 and β2 nAChR subunits (in a ratio 1:1), or rat α7 nAChR subunit along with chaperone NACHO (in a ratio 2:1). Oocytes were incubated at 18ºC in regular Barth's solution composed of (in mM) 88 NaCl, 1.1 KCl, 2.4 $NaHCO_3$, 0.3 $Ca(NO_3)_2$, 0.4 $CaCl_2$, 0.8 $MgSO_4$ and 15 HEPES-NaOH at pH 7.6, supplemented with 40 µg/mL gentamicin and 100 µg/mL ampicillin for 4-5 days before electrophysiological recordings. Two-electrode voltage clamp recordings were made using a turbo TEC-03X amplifier (Npi electronic, Germany) and Patch master software (HEKA, Germany), at a holding potential of -60 mV. Oocytes were briefly washed with normal frog Ringer's solution composed of (in mM) 115 NaCl, 2.5 KCl, 1.8 $CaCl_2$, 10 HEPES at pH 7.2 followed by an agonist application. Washout with normal frog Ringer's solution was done for 5 min between agonist applications. Oocytes expressing human α4β2 nAChR were pre-incubated with **1a**, **2a**, **3a**, or **6a** for 5 min followed by its co-application with nicotine. Peak current amplitudes of agonist-evoked responses were measured before and after pre-incubation of oocytes with **1a**, **2a**, **3a**, or **6a**. The ratio between these two measurements was used to assess the activity of compounds on human α4β2 nAChR. Data are presented as mean ± SEM for the indicated number of biological replicates (n). Statistical analysis (One-way ANOVA with Tukey's HSD test) was performed using OriginPro 9.0 software (OriginLab Corporation, Northampton, MA, USA). In the test, $p < 0.05$ was taken as significant.

Calcium imaging

Mouse neuroblastoma Neuro2a cells grown in black 96-well plate in DMEM (Paneco, Russia) supplemented with 10% FBS (ThermoFisher Scientific, USA) were transiently transfected with plasmids coding human α7 nAChR (α7 nAChR-pCEP4), chaperone NACHO (TMEM35-pCMV6-XL5, OriGene, USA) and a fluorescent calcium sensor Case12 (pCase12-cyto vector, Evrogen, Russia) following lipofectamine transfection protocol (Invitrogen, USA). The intracellular calcium concentration $[Ca^{2+}]_i$ measurements were performed on mouse neuroblastoma Neuro2a cells transfected with human α7 nAChR, using an already reported protocol.[26, 41] The procedure of calcium imaging was performed in a buffer containing 140 mM NaCl, 2 mM $CaCl_2$, 2.8 mM KCl, 4 mM $MgCl_2$, 20 mM HEPES, 10 mM glucose; pH 7.4. Transfected Neuro2a cells were incubated with α7 nAChR positive allosteric modulator PNU120596 (10 mM, Tocris, UK) for 20 min at room temperature before ligand addition.

Human neuroblastoma cells SH-SY5Y grown in DMEM/F12 medium (ThermoFisher Scientific, USA) supplemented with 10% fetal bovine serum (FBS) (ThermoFisher Scientific, USA), were plated at a density of 5000-10000 cells per well in a 96-well black plate (Corning, USA). Cells were grown in a CO_2 incubator for 48-72 h before testing the functional activity of natively expressed nAChRs by calcium imaging. SH-SY5Y cells were loaded with a fluorescent dye Fluo-4, AM (1.824 μM, ThermoFisher Scientific, USA) and a water-soluble probenecid (1.25 mM, ThermoFisher Scientific, USA) according to the manufacturer's protocol.

To test the agonistic properties compounds **1a**, **2a**, **3a** and **6a** were added immediately before measuring the fluorescence of the calcium sensor. Fluorescence of the calcium sensor was detected by the multimodal microplate reader Hidex Sence (Hidex, Turku, Finland) (ex/em = 485/535 nm) every 2s for three minutes. Responses were measured as peak intensity minus basal fluorescence one and were expressed as a percentage of the maximal response obtained to agonist. Data files were analyzed using Hidex Sence software (Hidex, Turku, Finland) and OriginPro 9.0 software (OriginLab, MA, USA).

Molecular Modeling

The CSD was scanned through the ConQuest search engine[28] using queries containing of the following elements:

(i) a (potentially cationic) nitrogen (N);

(ii) a hydrogen bond acceptor (N belonging to a heteroaromatic ring or O=C); a generic Qa atom (Qa=C,N) connected to the heteroaromatic nitrogen or to the carbonyl carbon

(iii) a plane defined by the C–N–Qa or C-(C=O)-Qa substructure.

(iv) the distance between potentially cationic nitrogen and the potential H-bond acceptor falling in the range 3.9-6.6

(v) the distance between potentially cationic nitrogen and the plane defined by the C–N–Qa or C-(C=O)-Qa substructure falling in the range 0.7-1.7.

The X-ray structure of the α4β2 receptor in complex with nicotine (pdb code 5KXI[31]) was prepared according to the Protein preparation wizard protocol in Maestro (v.10.5)[64a] that consists in the preliminary pre-treatment by adjusting the bond orders, evaluating the ionization states (Epik, v.3.5),[64b] adding hydrogen atoms, refining loop region (Prime, v.4.3)[64c] and energy minimization (Impact, v.7.0).[64d] 3D structures of diastereoisomers of compounds **1-10** were prepared using Maestro, evaluated for their ionization states at pH 7.4 ± 0.5 with Epik. OPLS-2005 force field in Macromodel[64e] was used for energy minimization for a maximum number of 2500 conjugate gradient iterations and setting a convergence criterion of 0.05 kcal $mol^{-1}Å^{-1}$. All docking computations were performed with the Glide program (v.7.0).[64f] Grids for docking were centered in the centroid of the complexed ligand, considering only one binding site, i.e. that one at chain D-E interface. The standard precision (SP) mode of the GlideScore function was applied to evaluate the predicted binding poses. The pictures were generated with Maestro.

ASSOCIATED CONTENT

Supporting Information

The Supporting Information is available free of charge on the ACS publications website http://pubs.acs.org.

Docked orientation of compounds **1a** and **1b** in the homology model of the α4β2 nicotinic receptor. Chemical structure of the enantiomers of compounds **1a** and **1b.** Predicted poses for the enantiomers of compound **1b** (*exo*) and **1a** (*endo*) and cognate nicotine in 5KXI. Calcium rise obtained with nicotine on α7 receptors expressed in neuroblastoma Neuro2a cell line. ^{1}H and ^{13}C NMR spectra of some selected *endo* compounds. Chromatographic profiles of LC-DAD analysis and corresponding UV spectra (PDF).

Molecular formula strings with pharmacological data (CSV).

AUTHOR INFORMATION

Corresponding author

E-mail: dina.manetti@unifi.it

ACKNOWLEDGMENTS

This work was supported by grants from MUR (PRIN 2009, 2009ESXPT2_002), from University of Florence (RICATEN15, RICATEN16) and Russian Foundation for basic Research (RFBR 18-04-00844).

ABBREVIATIONS USED

MLA, [^{3}H]-methyllycaconitine; SH-SY5Y, human neuroblastoma cell line; CSD, Cambridge Structural Database; PHT, pyrido[3,4]homotropane; abs, absolute; SEM, standard error of the mean; logBB, log blood/brain; NHEA, number of non-hydrogen atoms; HSD, Honestly Significant Difference; ANOVA, analysis of variance; FWHM, full width at half maximum; RDB, double bond/ring equivalents; HEPES, 4-(2-Hydroxyethyl)piperazine-1-ethanesulfonic acid; FBS, fetal bovine serum; DMEM, Dulbecco's Modified Eagle Medium; SP, standard precision.

REFERENCES

(1) Dineley, K. T.; Pandya, A. A.; Yakel, J. L. Nicotinic ACh receptors as therapeutic targets in CNS disorders. *Trends Pharmacol. Sci.* **2015**, *36* (2), 96-108.

(2) Quik, M.; Zhang, D.; McGregor, M.; Bordia, T. Alpha7 nicotinic receptors as therapeutic targets for Parkinson's disease. *Biochem. Pharmacol.* **2015**, *97* (4), 399-407.

(3) Quik, M.; Wonnacott, S. α6β2* and α4β2* nicotinic acetylcholine receptors as drug targets for Parkinson's disease. *Pharmacol. Rev.* **2011**, *63* (4), 938-966.

(4) Foucault-Fruchard, L.; Antier, D. Therapeutic potential of α7 nicotinic receptor agonists to regulate neuroinflammation in neurodegenerative diseases. *Neural Regen. Res.* **2017**, *12* (9), 1418-1421.

(5) Hone, A. J.; McIntosh, J. M. Nicotinic acetylcholine receptors in neuropathic and inflammatory pain. *FEBS Lett.* **2017**, 12884.

(6) Fujii, T.; Mashimo, M.; Moriwaki, Y.; Misawa, H.; Ono, S.; Horiguchi, K.; Kawashima, K. Expression and function of the cholinergic system in immune cells. *Front. Immunol.* **2017**, *8* (1085), 1-18.

(7) Zhao, Y. The oncogenic functions of nicotinic acetylcholine receptors. *J. Oncol.* **2016**, *2016*, (9), 1-9.

(8) Manetti, D.; Bellucci, C.; Chiaramonte, N.; Dei, S.; Teodori, E.; Romanelli, M. N. Designing selective modulators for the nicotinic receptor subtypes: challenges and opportunities. *Future Med. Chem.* **2018**, *10*, 433-459.

(9) Jensen, A. A.; Frølund, B.; Liljefors, T.; Krogsgaard-Larsen, P. Neuronal nicotinic acetylcholine receptors: structural revelations, target identifications, and therapeutic inspirations. *J. Med. Chem.* **2005**, *48*, 4705-4745.

(10) Coe, J. W.; Brooks, P. R.; Vetelino, M. G.; Wirtz, M. C.; Arnold, E. P.; Huang, J.; Sands, S. B.; Davis, T. I.; Lebel, L. A.; Fox, C. B.; Shrikhande, A.; Heym, J. H.; Schaeffer, E.; Rollema, H.; Lu, Y.; Mansbach, R. S.; Chambers, L. K.; Rovetti, C. C.; Schulz, D. W.; Tingley, F. D. I.; O'Neill, B. T. Varenicline: an α4β2 nicotinic receptor partial agonist for smoking cessation. *J. Med. Chem.* **2005**, *48*, 3474-3477.

(11) Mihalak, K. B.; Carroll, F. I.; Luetje, C. W. Varenicline is a partial agonist at α4β2 and a full agonist at α7 neuronal nicotinic receptors. *Mol. Pharmacol.* **2006**, *70* (3), 801-805.

(12) Brunzell, D. H.; McIntosh, J. M.; Papke, R. L. Diverse strategies targeting α7 homomeric and α6β2* heteromeric nicotinic acetylcholine receptors for smoking cessation. *Ann. N. Y. Acad. Sci.* **2014**, *1327* (1), 27-45.

(13) Bagdas, D.; Alkhlaif, Y.; Jackson, A.; Carroll, F. I.; Ditre, J. W.; Damaj, M. I. New insights on the effects of varenicline on nicotine reward, withdrawal and hyperalgesia in mice. *Neuropharmacology* **2018**, *138*, 72-79.

(14) Briggs, C. A.; Anderson, D. J.; Brioni, J. D.; Buccafusco, J. J.; Buckley, M. J.; Campbell, J. E.; Decker, M. W.; Donnelly-Roberts, D.; Elliott, R. L.; Gopalakrishnan, M.; Holladay, M. W.; Hui, Y.-H.; Jackson, W. J.; Kim, D. J. B.; Marsh, K. C.; O'Neill, A.; Prendergast, M. A.; Ryther, K. B.; Sullivan, J. P.; Arneric, S. P. Functional characterization of the novel neuronal nicotinic

acetylcholine receptor ligand GTS-21 in vitro and in vivo. *Pharmacol. Biochem. Behav.* **1997**, *57* (1-2), 231-241.

(15) Gotti, C.; Zoli, M.; Clementi, F. Brain nicotinic acetylcholine receptors: native subtypes and their relevance. *Trends Pharmacol. Sci.* **2006**, *27* (9), 482-491.

(16) Zoli, M.; Pistillo, F.; Gotti, C. Diversity of native nicotinic receptor subtypes in mammalian brain. *Neuropharmacology* **2015**, *96, Part B*, 302-311.

(17) Berrettini, W.; Yuan, X.; Tozzi, F.; Song, K.; Francks, C.; Chilcoat, H.; Waterworth, D.; Muglia, P.; Mooser, V. α-5/α-3 nicotinic receptor subunit alleles increase risk for heavy smoking. *Mol. Psychiatry* **2008**, *13*, 368-373.

(18) Caporaso, N.; Gu, F.; Chatterjee, N.; Sheng-Chih, J.; Yu, K.; Yeager, M.; Chen, C.; Jacobs, K.; Wheeler, W.; Landi, M. T.; Ziegler, R. G.; Hunter, D. J.; Chanock, S.; Hankinson, S.; Kraft, P.; Bergen, A. W. Genome-wide and candidate gene association study of cigarette smoking behaviors. *PLoS One* **2009**, *4* (2), e4653.

(19) Cuny, H.; Yu, R.; Tae, H.-S.; Kompella, S. N.; Adams, D. J. α-Conotoxins active at α3-containing nicotinic acetylcholine receptors and their molecular determinants for selective inhibition. *Br. J. Pharmacol.* **2018**, *175* (11), 1855-1868.

(20) Yuan, M.; Malagon, A. M.; Yasuda, D.; Belluzzi, J. D.; Leslie, F. M.; Zaveri, N. T. The α3β4 nAChR partial agonist AT-1001 attenuates stress-induced reinstatement of nicotine seeking in a rat model of relapse and induces minimal withdrawal in dependent rats. *Behav. Brain Res.* **2017**, *333* (Supplement C), 251-257.

(21) Khroyan, T. V.; Yasuda, D.; Toll, L.; Polgar, W. E.; Zaveri, N. T. High affinity α3β4 nicotinic acetylcholine receptor ligands AT-1001 and AT-1012 attenuate cocaine-induced conditioned place preference and behavioral sensitization in mice. *Biochem. Pharmacol.* **2015**, *97* (4), 531-541.

(22) Guandalini, L.; Martini, E.; Dei, S.; Manetti, D.; Scapecchi, S.; Teodori, E.; Romanelli, M. N.; Varani, K.; Greco, G.; Spadola, L.; Novellino, E. Design of novel nicotinic ligands through 3D database searching. *Bioorg. Med. Chem.* **2005**, *13*, 799-807.

(23) Kanne, D. B.; Abood, L. G. Synthesis and biological characterization of pyridohomotropanes. Structure-activity relationships of conformationally restricted nicotinoids. *J. Med. Chem.* **1988**, *31*, 506-509.

(24) Carroll, F. I.; Navarro, H. A.; Mascarella, S. W.; Castro, A. H.; Luetje, C. W.; Wageman, C. R.; Marks, M. J.; Jackson, A.; Damaj, M. I. In vitro and in vivo neuronal nicotinic receptor properties of (+)- and (−)-pyrido[3,4]homotropane [(+)- and (−)-PHT]: (+)-PHT is a potent and selective full agonist at α6β2 containing neuronal nicotinic acetylcholine receptors. *ACS Chem. Neurosci.* **2015**, *6* (6), 920-926.

(25) Guandalini, L.; Norcini, M.; Varani, K.; Pistolozzi, M.; Gotti, C.; Bazzicalupi, C.; Martini, E.; Dei, S.; Manetti, D.; Scapecchi, S.; Teodori, E.; Bertucci, C.; Ghelardini, C.; Romanelli, M. N. Design, synthesis, and preliminary pharmacological evaluation of new quinoline derivatives as nicotinic ligands. *J. Med. Chem.* **2007**, *50* (20), 4993-5002.

(26) Manetti, D.; Bellucci, C.; Dei, S.; Teodori, E.; Varani, K.; Spirova, E.; Kudryavtsev, D.; Shelukhina, I.; Tsetlin, V.; Romanelli, M. N. New quinoline derivatives as nicotinic receptor modulators. *Eur. J. Med. Chem.* **2016**, *110*, 246-258.

(27) Glennon, R. A.; Dukat, M. α4β2 nACh receptor pharmacophore models. *Bioorg. Med. Chem. Lett.* **2004**, *14*, 1841-1844.

(28) Allen, F. H. The Cambridge Structural Database: a quarter of a million crystal structures and rising. *Acta Crystallogr.* **2002**, *B58*, 380-388. The CSD version used in this work was updated in 2012.

(29) Dallanoce, C.; Grazioso, G.; Pomè, D. Y.; Sciaccaluga, M.; Matera, C.; Gotti, C.; Fucile, S.; De Amici, M. Investigating the hydrogen-bond acceptor site of the nicotinic pharmacophore model:

a computational and experimental study using epibatidine-related molecular probes. *J. Comput. Aided Mol. Des.* **2013**, *27* (11), 975-987.

(30) Matera, C.; Quadri, M.; Sciaccaluga, M.; Pomè, D. Y.; Fasoli, F.; De Amici, M.; Fucile, S.; Gotti, C.; Dallanoce, C.; Grazioso, G. Modification of the anabaseine pyridine nucleus allows achieving binding and functional selectivity for the α3β4 nicotinic acetylcholine receptor subtype. *Eur. J. Med. Chem.* **2016**, *108*, 392-405.

(31) Morales-Perez, C. L.; Noviello, C. M.; Hibbs, R. E. X-ray structure of the human α4β2 nicotinic receptor. *Nature* **2016**, *538*, 411-415.

(32) Walsh, R. M.; Roh, S.-H.; Gharpure, A.; Morales-Perez, C. L.; Teng, J.; Hibbs, R. E. Structural principles of distinct assemblies of the human α4β2 nicotinic receptor. *Nature* **2018**, *557* (7704), 261-265.

(33) Sgrignani, J.; Bonaccini, C.; Grazioso, G.; Chioccioli, M.; Cavalli, A.; Gratteri, P. Insights into docking and scoring neuronal alpha4beta2 nicotinic receptor agonists using molecular dynamics simulations and QM/MM calculations. *J. Comput. Chem.* **2009**, *30*, 2443-2454.

(34) Bourguignon, J.; Le Nard, G.; Queguiner, G. Synthèse d'aryl nitronorbonènes par cycloaddtion de Diels-Alder entre les aryl-nitroéthylènes et le cyclopentadiène. Justification de la stéréochimie et de la réactivité relative observes par la method CNDO/II. Obtention d'aryl aminonorbornènes. *Can. J. Chem.* **1985**, *63*, 2354-2361.

(35) Pandey, G.; Bagul, T. D.; Sahoo, A. K. [3 + 2] Cycloaddition of nonstabilized azomethine ylides. 7. Stereoselective synthesis of epibatidine and analogues. *J. Org. Chem.* **1998**, *63* (3), 760-768.

(36) Duursma, A.; Minnaard, A. J.; Feringa, B. L. One-pot multi substrate enantioselective conjugate addition of diethylzinc to nitroalkenes. *Tetrahedron* **2002**, *58*, 5773-5778.

(37) Cochhran, T. G.; Huitric, A. C. The use of nuclear magnetic resonance as a monitor in optical resolutions. The synthesis and resolution of cis- and trans-2-(o-bromophenyl)cyclohexylamines. *J. Org. Chem.* **1971**, *36*, 3046-3048.

(38) Gao, Y.; Kellar, K. J.; Yasuda, R. P.; Tran, T.; Xiao, Y.; Dannals, R. F.; Horti, A. G. Derivatives of dibenzothiophene for position emission tomography imaging of α7-nicotinic acetylcholine receptors. *J. Med. Chem.* **2013**, *56*, 7574-7589.

(39) Glennon, R. A.; Dukat, M. Central nicotinic receptor ligands and pharmacophores. *Pharm. Acta Helv.* **2000**, *74* (2), 103-114.

(40) Post, M. R.; Tender, G. S.; Lester, H. A.; Dougherty, D. A. Secondary ammonium agonists make dual cation-π interactions in α4β2 nicotinic receptors. *eNeuro,*2017, *4* (2), 1-8.

(41) Shelukhina, I. V.; Zhmak, M. N.; Lobanov, A. V.; Ivanov, I. A.; Garifulina, A. I.; Kravchenko, I. N.; Rasskazova, E. A.; Salmova, M. A.; Tukhovskaya, E. A.; Rykov, V. A.; Slashcheva, G. A.; Egorova, N. S.; Muzyka, I. S.; Tsetlin, V. I.; Utkin, Y. N. Azemiopsin, a selective peptide antagonist of muscle nicotinic acetylcholine receptor: preclinical evaluation as a local muscle relaxant. *Toxins* **2018**, *10*, 34.

(42) Hopkins, A. L.; Groom, C. R.; Alex, A. Ligand efficiency: a useful metric for lead selection *Drug Discovery Today* **2004**, *9*, 430-431.

(43) Hopkins, A. L.; Keserü, G. M.; Leeson, P. D.; Rees, D. C.; Reynolds, C. H. The role of ligand efficiency metrics in drug discovery. *Nat. Rev. Drug Disc.* **2014**, *13*, 105-121.

(44) Ghose, A. K.; Herbertz, T.; Hudkins, R. L.; Dorsey, B. D.; Mallamo, J. P. Knowledge-based, central nervous system (CNS) lead selection and lead optimization for CNS drug discovery. *ACS Chem. Neurosci.* **2012**, *3* (1), 50-68.

(45) Clark, D. E. Rapid calculation of polar molecular surface area and its application to the prediction of transport phenomena. 2. Prediction of blood-brain barrier penetration. *J. Pharm. Sci.* **1999**, *88*, 815-821.

(46) Abraham, M. H.; Chadha, H. S.; Mitchell, R. C. Hydrogen bonding. 33. Factors that influence the distribution of solutes between blood and brain *J. Pharm. Sci.* **1994**, *83*, 1257-1268.

(47) Yamauchi, J. G.; Nemecz, A.; Nguyen, Q. T.; Muller, A.; Schroeder, L. F.; Talley, T. T.; Lindstrom, J.; Kleinfeld, D.; Taylo, P. Characterizing ligand-gated ion channel receptors with genetically encoded Ca2++ sensors. *PLoS One* **2011**, *6* (1), e16519.

(48) Hurst, R. S.; Hajos, M.; Raggenbass, M.; Wall, T. M.; Higdon, N. R.; Lawson, J. A.; Rutherford-Root, K. L.; Berkenpas, M. B.; Hoffmann, W. E.; Piotrowski, D. W.; Groppi, V. E.; Allaman, G.; Ogier, R.; Bertrand, S.; Bertrand, D.; Arneric, S. P. A novel positive allosteric modulator of the alpha7 neuronal nicotinic acetylcholine receptor: *in vitro* and *in vivo* characterization. *J. Neurosci.* **2005**, *25*, 4396-4405.

(49) Szabo, A. K.; Pesti, K.; Mike, A.; Vizi, E. S. Mode of action of the positive modulator PNU-120596 on alpha7 nicotinic acetylcholine receptors. *Neuropharmacology* **2014**, *81*, 42-54.

(50) Young, G. T.; Zwart, R.; Walker, A. S.; Sher, E.; Millar, N. S. Potentiation of alpha7 nicotinic acetylcholine receptors via an allosteric transmembrane site. *Proc. Natl. Acad. Sci. U. S. A.* **2008**, *105*, 14686-14691.

(51) Wang, F.; Gerzanich, V.; Wells, G. B.; Anand, R.; Peng, X.; Keyser, K.; Lindstrom, J. Assembly of human neuronal nicotinic receptor α5 subunits with α3, β2, and β4 subunits. *J. Biol. Chem.* **1996**, *271* (30), 17656-17665.

(52) de la Fuente Revenga, M.; Balle, T.; Jensen, A. A.; Frølund, B. Conformationally restrained carbamoylcholine homologues. Synthesis, pharmacology at neuronal nicotinic acetylcholine receptors and biostructural considerations. *Eur. J. Med. Chem.* **2015**, *102*, 352-362.

(53) Charton, Y.; Guillonneau, C.; Lockhart, B.; Lestage, P.; Goldstein, S. Preparation and affinity profile of novel nicotinic ligands. *Bioorg. Med. Chem. Lett.* **2008**, *18* (6), 2188-2193.

(54) Schrimpf, M. R.; Sippy, K. B.; Daanen, J. F.; Ryther, K. B.; Ji, J. Heterocyclic Substituted Aminoazacycles Useful as Central Nervous System Agents. EP1428824 (A1) **2004**.

(55) Nirogi, R.; Mohammed, A. R.; Kumawat, K. R.; Ahmad, I.; Jayarajan, P.; Shinde, A. K.; Kandikere, N. V.; Mudigonda, K.; Jasti, V. α4β2 Neuronal Nicotinic Acetylcholine Receptor Ligands. WO2011080751 (A2) **2011**.

(56) Carroll, F. I.; Brieaddy, L. E.; Navarro, H. A.; Damaj, M. I.; Martin, B. R. Synthesis and pharmacological characterization of exo-2-(2'-chloro-5-pyridinyl)-7-(endo and exo)-

aminobicyclo[2.2.1]heptanes as novel epibatidine analogues. *J. Med. Chem.* **2005**, *48* (23), 7491-7495.

(57) Kasheverov, I.; Shelukhina, I.; Kudryavtsev, D.; Makarieva, T.; Spirova, E.; Guzii, A.; Stonik, V.; Tsetlin, V. 6-Bromohypaphorine from marine nudibranch mollusk hermissenda crassicornis is an agonist of human α7 nicotinic acetylcholine receptor. *Mar. Drugs* **2015**, *13* (3), 1255-1266.

(58) Azam, L.; McIntosh, J. M. Molecular basis for the differential sensitivity of rat and human α9α10 nAChRs to α-conotoxin RgIA. *J. Neurochem.* **2012**, *122* (6), 1137-1144.

(59) Shelukhina, I.; Spirova, E.; Kudryavtsev, D.; Ojomoko, L.; Werner, M.; Methfessel, C.; Hollmann, M.; Tsetlin, V. Calcium imaging with genetically encoded sensor Case12: facile analysis of α7/α9 nAChR mutants. *PLoS One* **2017**, *12* (8), e0181936.

(60) Milstein, D. Addition of Aldehydes to Organic Compounds Having a Carbon-Hydrogen Bond Activated by a Nitro or Nitrile Group. US4581178, **1986**.

(61) Romanelli, M. N.; Manetti, D.; Scapecchi, S.; Borea, P. A.; Dei, S.; Bartolini, A.; Ghelardini, C.; Gualtieri, F.; Guandalini, L.; Varani, K. Structure-affinity relationships of a unique nicotinic ligand: N^1-dimethyl-N^4-phenylpiperazinium iodide (DMPP). *J. Med. Chem.* **2001**, *44*, 3946-3955.

(62) Davies, A. R.; Hardick, D. J.; Blagbrough, I. S.; Potter, B. V.; Wolstenholme, A. J.; Wonnacott, S. Characterisation of the binding of [3H]methyllycaconitine: a new radioligand for labelling α7-type neuronal nicotinic acetylcholine receptors. *Neuropharmacology* **1999**, *38* (5), 679-690.

(63) Wilkins, L. H. J.; Grinevich, V. P.; Ayers, J. T.; Crooks, P. A.; Dwoskin, L. P. N-n-Alkylnicotinium analogs, a novel class of nicotinic receptor antagonists: interaction with α4β2* and α7* neuronal nicotinic receptors. *J. Pharmacol. Exp. Ther.* **2003**, *304*, 400-410.

(64) *Schrödinger Suite Release 2016-1, Schrödinger, LLC, New York, NY, 2016*, New York, 2016. (a) Maestro v.10.5; (b) Epik, v.3.5; (c) Impact, v.7.0; (d) Prime, v.4.3; (e) Macromodel v.11.1. (f) Glide, v.7.0.

Table of Contents graphic